An Essential Pentatricopeptide Repeat Protein Facilitates 5′ Maturation and Translation Initiation of *rps3* mRNA in Maize Mitochondria [C][W]

Nikolay Manavski,[a,b] Virginie Guyon,[c] Jörg Meurer,[b] Udo Wienand,[a] and Reinhold Brettschneider[a,1]

[a] Biozentrum Klein Flottbek und Botanischer Garten, Universität Hamburg, 22609 Hamburg, Germany
[b] Biozentrum der Ludwig-Maximillians-Universität München, Plant Molecular Biology/Botany, 82152 Planegg-Martinsried, Germany
[c] Cereal Genetics and Genomics, Biogemma Société par Actions Simplifiées, 63720 Chappes, France

Pentatricopeptide repeat (PPR) proteins are members of one of the largest nucleus-encoded protein families in plants. Here, we describe the previously uncharacterized maize (*Zea mays*) PPR gene, *MPPR6*, which was isolated from a *Mutator*-induced collection of maize kernel mutants by a cDNA-based forward genetic approach. Identification of a second mutant allele and cosegregation analysis confirmed correlation with the mutant phenotype. Histological investigations revealed that the mutation coincides with abnormities in the transfer cell layer, retardation of embryo development, and a considerable reduction of starch level. The function of MPPR6 is conserved across a wide phylogenetic distance as revealed by heterologous complementation of the *Arabidopsis thaliana* mutant in the orthologous *APPR6* gene. MPPR6 appeared to be exclusively present in mitochondria. RNA coimmunoprecipitation and in vitro binding studies revealed a specific physical interaction of MPPR6 with the 5′ untranslated region of *ribosomal protein S3* (*rps3*) mRNA. Mapping of transcript termini showed specifically extended *rps3* 5′ ends in the *mppr6* mutant. Considerable reduction of mitochondrial translation was observed, indicating loss of RPS3 function. This is consistent with the appearance of truncated RPS3 protein lacking the N terminus in *mppr6*. Our results suggest that MPPR6 is directly involved in 5′ maturation and translation initiation of *rps3* mRNA.
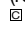
INTRODUCTION

In the mature embryo sac of maize (*Zea mays*), double fertilization initiates the development of the embryo and endosperm. The fusion of the sperm and egg nuclei forms the zygote from which the proembryo and later on the embryo develops. The triploid primary endosperm arises from the fusion of the second sperm nucleus with the two polar nuclei. These undergo several mitotic divisions resulting in up to 512 free nuclei. Cell wall formation leads the endosperm to become cellular (Kiesselbach, 1949). Shortly thereafter, cells of the endosperm begin to differentiate, forming four distinct tissue types: aleurone, central starchy endosperm, embryo surrounding region (ESR), and basal endosperm transfer layer (BETL). The outermost epidermal single cell layer, the aleurone, provides enzymes required for hydrolysis of starch and storage proteins, which make up the main content of the central endosperm of cereals. The ESR forms the cavity in which the embryo is located, whereas the BETL constitutes the base of the endosperm and is adjacent to the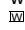 maternal pedicel. Both the ESR and BETL tissue types supply the embryo with nutrients and are therefore thought to be required for seed development.

In maize, a mature dormant seed with a well-developed embryo and starchy endosperm is the normal product of fertilization. Variations from this norm with significantly reduced embryo or endosperm development are considered as defective kernel types (Lowe and Nelson, 1946). Normal grain filling and development depends on mitochondrial function (Kang et al., 2009) and sufficient nutrient supply, which in turn depends on appropriate differentiation and function of cells, such as BETL cells, specialized for the transport of solutes (Thompson et al., 2001; Royo et al., 2007).

The endosymbiotic hypothesis suggests that mitochondria are descendants of α-proteobacteria. Over time, most of the endosymbiotic genes have been either lost or transferred to the nucleus. According to estimates, the mitochondrial proteome of vascular plants is composed of 2000 to 3000 proteins (reviewed in Millar et al., 2005), the majority of which are encoded in the nucleus. Only a limited number of gene products are encoded in the plant mitochondrial genome, and most of them are necessary for building up ribosomes and the respiratory chain. Expression and regulation of these genes is subjected to various posttranscriptional steps in which many nuclear-encoded proteins are involved. A recently discovered RNA binding pentatricopeptide repeat (PPR) protein family is considered to play a central role in these processes (reviewed in Schmitz-Linneweber and Small, 2008). PPR proteins are characterized by the presence of tandem arrays of a degenerate 35–amino acid residue repeat. The PPR motif is predicted to consist of two antiparallel

α-helices, which in tandem arrays form a superhelical structure enclosing a hydrophilic, positively charged groove supposed to bind hydrophilic, acidic ligands, such as RNA (Small and Peeters, 2000; Kobayashi et al., 2012). Members of the huge PPR protein family are particularly found in plant organelles. A total of 441 members are present in *Arabidopsis thaliana*, the majority of which is encoded by single exon genes (Lurin et al., 2004). So far characterized PPR proteins have been implicated in quite diverse posttranscriptional steps, such as RNA editing (Kotera et al., 2005; Okuda et al., 2006; Chateigner-Boutin et al., 2008; Bentolila et al., 2010; Sung et al., 2010; Uchida et al., 2011; Hammani et al., 2011), RNA splicing (Schmitz-Linneweber et al., 2006; de Longevialle et al., 2007; Hattori et al., 2007; Koprivova et al., 2010; Liu et al., 2010; Chateigner-Boutin et al., 2011), RNA stability (Beick et al., 2008; Pfalz et al., 2009; Johnson et al., 2010; Pusnik and Schneider, 2012), RNA processing (Meierhoff et al., 2003; Jonietz et al., 2010, 2011; Hölzle et al., 2011) and translation (Schmitz-Linneweber et al., 2005; Uyttewaal et al., 2008, Prikryl et al., 2011; Cai et al., 2011). Despite the obvious recent progress in understanding their key role, little is known about their exact biological function. Therefore, further studies of PPR proteins and their ligands are required to elucidate their molecular function and specific targets.

In this work, we describe the genetic and molecular characterization of a gene encoding a PPR protein essential for kernel development in maize, which we named maize *PPR6* (*MPPR6*). A mutation in *MPPR6* caused by the insertion of a *Mu1.7* transposon element creates a defective kernel phenotype associated with retarded grain development and filling, as well as morphological alterations of the BETL. The identification of one additional *mppr6* allele in maize showing the same phenotype confirmed that *mppr6* is causal for the mutant phenotype. We further demonstrate that the *mppr6*-related phenotype of the *Arabidopsis ppr6* (*appr6*) T-DNA insertion line can be functionally complemented by heterologous expression of the *MPPR6* gene, demonstrating a remarkably conserved function among land plants. Similar kernel defects in maize were described in knockouts of the mitochondria-targeted PPR protein Empty Pericarp4 (EMP4) required for accumulation of a certain set of mitochondrial transcripts. However, the precise function and targets of EMP4 remained unclear (Gutiérrez-Marcos et al., 2007). Our data show that *mppr6* is specifically affected in posttranscriptional expression of the *ribosomal protein S3* (*rps3*) gene in mitochondria. MPPR6 is associated in vivo with the 5′ untranslated region (UTR) of mitochondrial (*rps3*) mRNA, consistent with its proposed function in accurate *rps3* 5′ maturation and translation initiation.

RESULTS

Analysis of the *mppr6* Mutant Phenotype

The maize *mppr6* mutant originates from Biogemma's collection of *Mutator* (*Mu*) transposon-induced defective kernel mutants. In immature heterozygous *mppr6* (*mppr6*/+) ears, the recessive seed mutation is macroscopically visible at around 11 d after pollination (DAP). Approximately one-quarter of the kernels appeared small, pale, and distorted (Figure 1A; see Supplemental Figure 1D online). Embryos dissected from 18 DAP homozygous *mppr6* (*mppr6*/−) kernels showed a small size and had a slightly translucent appearance (Figure 1B). Moreover, mutant embryos exhibited deformities at a later developmental stage (30 DAP), presumably caused by the pressure of adjacent wild-type kernels (Figure 1C). Since mature *mppr6*/− seeds did not germinate, we tried to recover embryos at 18 DAP from immature kernels and investigated growth on Murashige and Skoog (MS) medium. In contrast with wild-type plants, rescued *mppr6*/− individuals grew much slower but were able to grow further on soil (Figure 1D). However, alongside the pronounced dwarfism (maximal 20 cm; see Supplemental Figures 1A and 1B online) in the homozygous *mppr6* mutant plants, male flowers were lacking and replaced by a female one.

To investigate the mutant phenotype closely, wax longitudinal sections of the *mppr6*/− and wild-type kernels at 12 DAP were
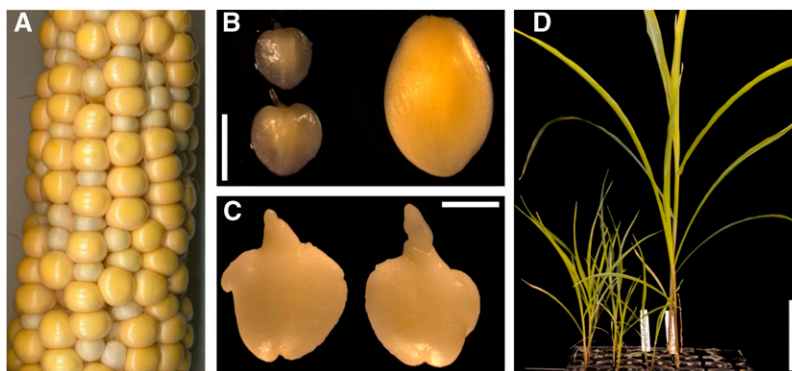
Figure 1. Phenotype of the *Mu*-Induced *mppr6* Mutant.

(A) A 25 DAP ear segregating for mutant and wild-type kernels obtained by self-pollination of a plant heterozygous for the *mppr6* mutation.
**(B)** Comparison between mutant (left) and wild-type (right) embryos at 18 DAP.
(C) The size of *mppr6*/− embryos at 30 DAP in **(C)** is comparable to that of the 18 DAP wild-type ones in **(B)**.
(D) Comparison between developing *mppr6* homozygous (left) and wild-type (right) rescued plants.
Bars = 1 mm in **(B)** and **(C)** and 10 cm in **(D)**.

stained with Azure B and examined microscopically. Both the embryo and endosperm were affected in *mppr6* mutants. A comparison between wild-type and mutant embryos revealed a significant developmental retardation of homozygous *mppr6* embryos (Figures 2A and 2B). In wild-type seeds, the endosperm entirely filled the pericarp (Figure 2A), whereas the size of the mutant endosperm was notably reduced, resulting in a gap between the pericarp and the aleurone (Figure 2B). Furthermore, the BETL was fragmented by structurally irregular cells devoid of wall ingrowths (WIGs) shown in Figures 2C and 2D. In fact, most of the *mppr6/−* BETL cells displayed relatively weak WIG formation (Figures 2E and 2F). A similar WIG phenotype was described in two further loss-of-function alleles of kernel mutants (Costa et al., 2003; Kang et al., 2009).
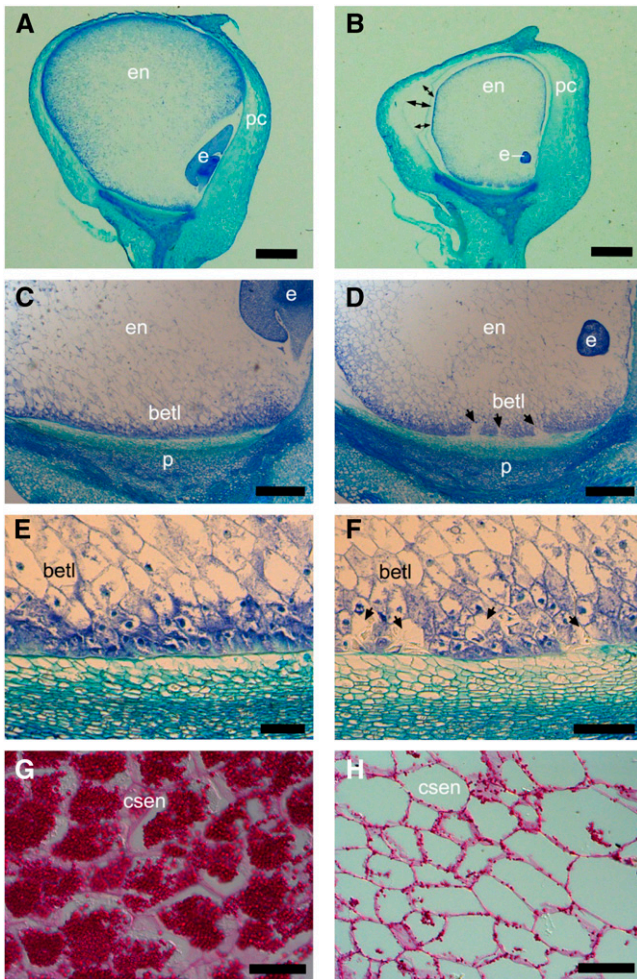
Figure 2. Embryo and Endosperm Are Altered in *mppr6* Mutant Kernels.

The 12-μm longitudinal wax sections of mutant (**[B]**, **[D]**, **[F]**, and **[H]**) and wild-type (**[A]**, **[C]**, **[E]**, and **[G]**) kernels at 12 DAP stained with Azure B (**[A]** to **[F]**) and periodic acid Schiff's reagent (**[G]** and **[H]**). In **(B)**, double arrows indicate the gap between pericarp and aleurone, whereas arrows in **(D)** and **(F)** show abnormal cells in the BETL. csen, central starchy endosperm; e, embryo; en, endosperm; p, pedicel; pc, pericarp. Bars = 1 mm in **(A)** and **(B)**, 100 μm in **(C)** and **(D)**, 60 μm in **(E)** and **(F)**, and 40 μm in **(G)** and **(H)**.

Starch levels in the endosperm were investigated by staining sections with periodic acid Schiff's reagent. A considerable starch reduction in mutant kernels was observed at 12 DAP (Figures 2G and 2H).

Molecular Cloning, Gene Structure, and Sequence Analysis of *MPPR6*

Genomic sequences flanking the *Mu* transposon and cosegregating with the *mppr6* mutant phenotype were identified using a new cDNA-based transposon display technique. In this procedure, total RNA extracted from mutant kernels of two segregating sibling ears and wild-type kernels of a single sibling wild-type ear was used for cDNA synthesis according to the rapid amplification of cDNA ends (RACE) protocol (Clontech). Reactions for 3′ and 5′ RACE were conducted using a *Mu*-specific primer paired with an adapter primer corresponding to the attached sequence at the end of the cDNA. All primer sequences used in this work are provided in Supplemental Table 1 online. To increase the specificity of displayed bands, a first round RACE was followed by a nested RACE reaction. A *Mu* flanking cDNA sequence of 1 kb was present in the 3′ RACE of both mutant samples but absent in the wild-type and therefore considered for cosegregation analysis (data not shown). Sequencing identified the 1-kb *Mu*-adjacent cDNA fragment as part of a PPR protein-encoding gene, named *MPPR6*. Further analysis revealed that the *mppr6* allele contains a *Mu1.7* element located in its open reading frame (ORF). The *Mu* element was flanked by 9-bp direct repeats, known as *Mu* target site duplication.

Genomic DNA extracted from leaf samples of 280 randomly selected sibling plants was sorted into segregating *mppr6/+* and wild-type plants according to the ear phenotype of self-pollinated plants. A PCR-based cosegregation analysis using a *Mu* and an *MPPR6*-specific primer indicated precise cosegregation with all 200 mutant plants and no linkage with 80 wild-type sibling individuals. An example of these results is shown in Figure 3A for 10 mutant and 10 wild-type samples.

To verify the PCR-based cosegregation, a DNA gel blot analysis was performed. Genomic DNA from 10 *mppr6/+* and 10 wild-type randomly chosen plants was digested with *Sac*I, which should result in a polymorphism when using an *MPPR6*-specific probe for hybridization (position of the probe is diagrammed in Figure 4A). A shift corresponding to the *Mu1.7* insertion was obtained after hybridization in all mutant samples but not in the wild type (Figure 3B). Consistent with the *Mu* insertion, the *mppr6* cDNA could not be amplified by RT-PCR in the mutants (Figure 3C).

To confirm that the *Mu* insertion into the *MPPR6* gene accounts for the phenotype, a *Mu*-induced mutant collection was screened for an additional *mppr6* allele (see Methods). An independent insertion event was successfully recovered. The second allele, which we named *mppr6-2*, contains a so far uncharacterized *Mu* element in the ORF of *MPPR6* 394 bp downstream of the start codon (Figure 4A) and shows an *mppr6*-like kernel phenotype. Allelic crosses between *mppr6-1/+* and *mppr6-2/+* resulted in ears segregating for normal and defective seeds in the expected 3:1 ratio, confirming that the mutant
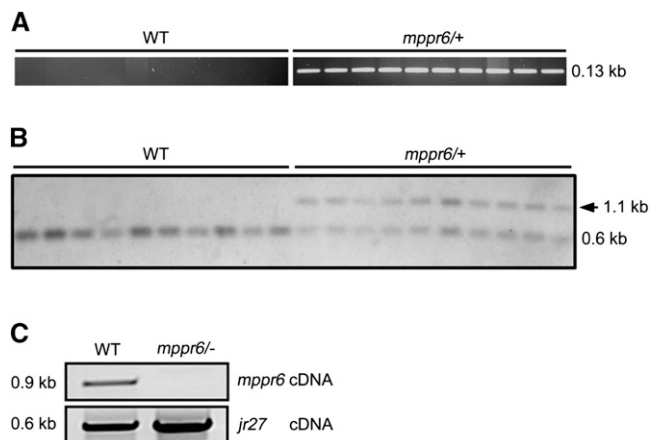
Figure 3. The *Mu* Insertion within *MPPR6* Cosegregates with the Mutant Phenotype.

(A) Cosegregation analysis by genomic PCR with *MPPR6*- and *Mu*-specific primers in the wild type (WT) and *mppr6/−* mutant.
(B) DNA gel blot hybridized with *MPPR6*-specific probe. The shift cosegregating with the *Mu1.7* insertion in the *mppr6/+* samples is indicated by an arrow (~1.1 kb).
(C) A wild-type copy of *mppr6* mRNA is absent in *mppr6* mutants. RNA from wild-type and *mppr6/−* embryos was reverse transcribed and *mppr6* mRNA was examined by RT-PCR using primer mppr6_1fw and mppr6_2rev, which flanks the *Mu1.7* element. The quality of the cDNA was analyzed by amplifying the mRNA of the ubiquitous expressed gene *jr27* (Lorbiecke et al., 2005) shown in the panel below.

phenotype of *mppr6-1* and *mppr6-2* is indeed the result of the *Mu* insertion in the *MPPR6* gene and that both mutants are allelic (see Supplemental Figure 1C online).

A full-length *mppr6* cDNA was generated by RACE using gene-specific primers. The cDNA consists of 1976 bp and a 5′ UTR of 201 bp followed by a 1470-bp-long ORF. The poly(A) tail is located 305 bp downstream of the stop codon (Figure 4A). Alignment of the cDNA to the corresponding genomic DNA sequence (MAGIv4_67802) revealed that the *MPPR6* gene contains a single exon. The *MPPR6* gene is located at the bottom of chromosome 1 and corresponds to the filter gene set GRMZM2G389645 that maps at position 279,177,101…279178807 on RefGen_V2. The deduced protein with a molecular mass of 55 to kD is composed of 489 amino acid residues and belongs to the P subclass of the PPR protein family. The 10 PPR domains stretch from amino acid residue 105 to 451. BLAST comparisons of protein sequences detected the putative orthologs in *Arabidopsis* and rice (*Oryza sativa*), At1g77360 (APPR6) and Os03g55340.1 (OPPR6), respectively. MPPR6 shares 97 and 80% similarity with OPPR6 and APPR6, respectively (Figure 4C). The proteins carry a predicted N-terminal mitochondrial transit peptide and share a highly conserved PPR motif structure (Figures 4B and 4C).

Genetic Complementation of the *appr6* Mutation with *MPPR6*

The functional relationship between the maize and *Arabidopsis* orthologs was investigated in a reverse genetics approach in

Arabidopsis. Three transgenic *Arabidopsis* lines, SALK_045714 (*appr6-1*), SALK_091917 (*appr6-2*), and SALK_061950 (*appr6-3*), containing a T-DNA insertion in the *APPR6* gene were obtained from the Salk Institute (http://signal.salk.edu/cgi-bin/tdnaexpress). Sequence analysis revealed that the T-DNAs in all three lines are inserted into the *APPR6* gene and that the insertion in *appr6-1* and *appr6-2* is located at the same position (1435 bp downstream of the start codon; Figure 4A). Seeds from each line were sown on soil and seedlings were genotyped. For all lines, only three-quarters of the seeds were able to germinate and no homozygous mutant plants were found. One-quarter of the seeds within developing siliques of plants heterozygous for the mutations appeared translucent and exhibited a significantly delayed embryo growth (Figure 5A). Moreover, ~25% of the mature dried seeds from heterozygous plants were small, shrunken (Figure 5B; see Supplemental Figure 1D online), and failed to germinate on soil. When grown on Suc-supplemented medium, homozygous *appr6* plants showed delayed growth (Figure 5C) and were able to grow further on soil although severely retarded. Nevertheless, *appr6* plants were able to reach reproductive maturity although still showing reduced size of inflorescences and siliques compared with those of the wild type.

Owing to sequence similarity and the related phenotype in maize and *Arabidopsis*, we performed a genetic complementation of the *appr6* mutation using the *MPPR6* gene. For that purpose, the PCR-amplified ORF of maize *MPPR6* was inserted into the binary vector pCHF5 downstream of the cauliflower mosaic virus 35S promoter (*35S:mppr6*; Figure 6A) and introduced into *appr6-3/+* plants using the *Agrobacterium tumefaciens*–mediated floral dip transformation method (Clough and Bent, 1998). In the T1 generation, three independent homozygous *appr6-3/−* plants harboring the *MPPR6* transgene were obtained (the results of one of these complemented plants is shown in Figures 6B and 6C). The phenotype and growth of these plants were indistinguishable from that of the wild type (Figure 6C). Genetic complementation proved that the *appr6* mutant phenotype was indeed caused by the T-DNA insertion in At1g77360. Most importantly, heterologous expression provides genetically proven evidence of cross-species conservation of PPR function among monocot and dicot plants.

Tissue-Specific Expression and Subcellular Localization of MPPR6

Due to the fact that the *mppr6* mutation primarily affects kernel development and could partially be overcome by growth on Suc during early development, we hypothesized that *MPPR6* is mainly expressed in kernel tissue. To test this, we examined the expression of *MPPR6* in several maize tissues by RNA gel blot analysis. However, no hybridization signal could be detected, indicating very low gene expression. Therefore, we analyzed accumulation of *mppr6* mRNA by RT-PCR (Figure 7). *MPPR6* was found to be primarily expressed in kernel and embryo tissue (0 to 21 DAP), but weak signals were also obtained in endosperm, leaves, seedlings, pollen, and roots.

We used TargetP (http://www.cbs.dtu.dk/services/TargetP/) (Emanuelsson et al., 2000) and Predotar (Small et al., 2004) to
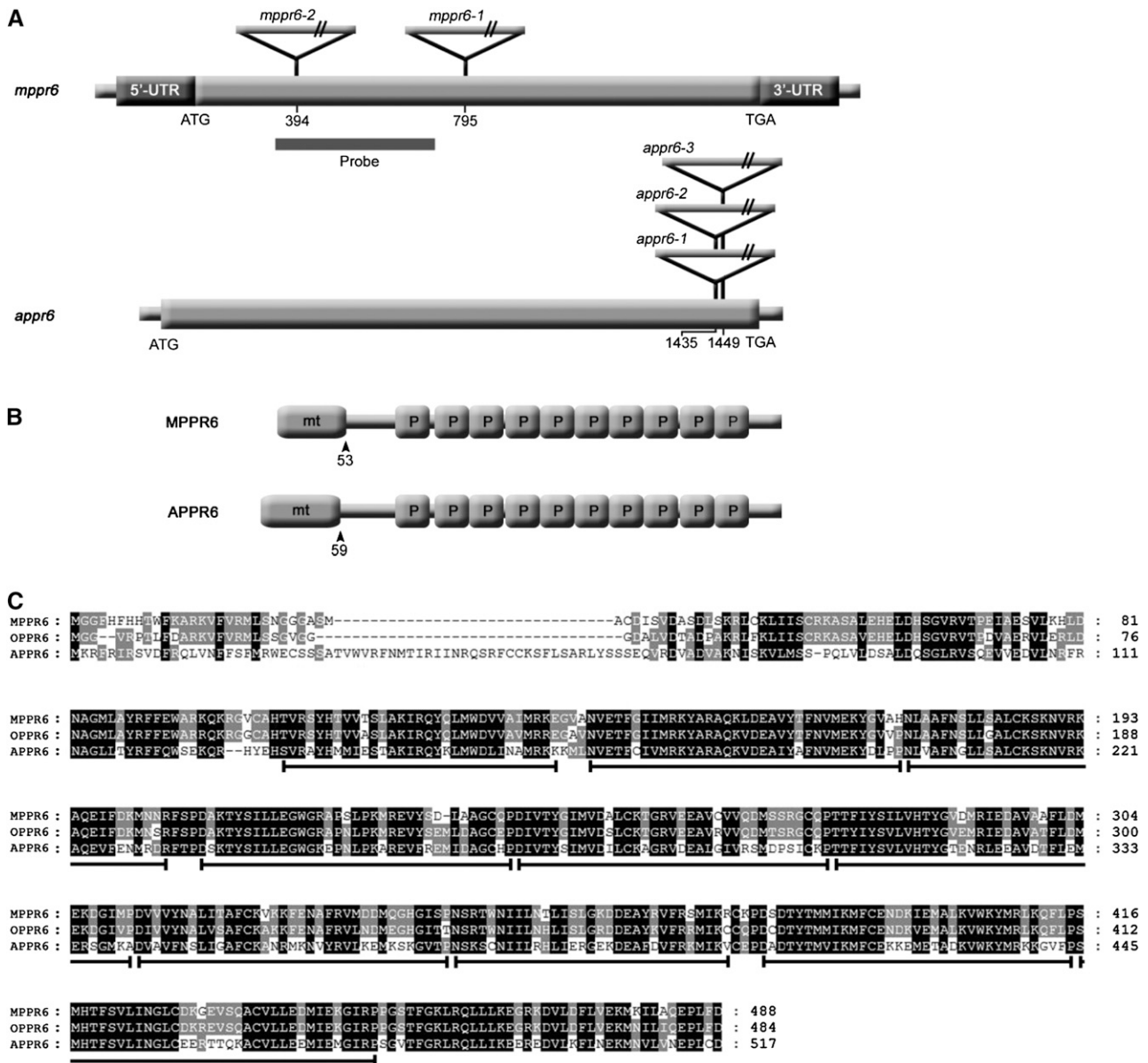
**Figure 4.** cDNA and Protein Structure of MPPR6 and APPR6.

(A) Schematic representation of *mppr6* and *appr6* cDNAs (diagrams not to scale). *Mu* (maize) and T-DNA insertions (*Arabidopsis*) are indicated by triangles. Positions of insertions with respect to the start codon (ATG) are shown in both cDNAs. ORFs are represented by wide gray bars, whereas dark-gray bars indicate the 5′ and 3′ UTRs in *mppr6* cDNA.

(B) Protein motif organization of MPPR6 and APPR6. Mitochondrial targeting signals (mt) and PPR motifs (P) are indicated. Amino acid positions of transit peptide cleavage sites are shown by arrowheads.

(C) Alignment of MPPR6 (maize), OPPR6 (rice), and APPR6 (*Arabidopsis*) orthologs. The homologous areas are highlighted. PPR motifs in the sequences are indicated below by black lines.

predict the subcellular localization of MPPR6. Both programs detected a putative mitochondrial transit peptide. To verify experimentally the predicted mitochondrial localization, the first 80 amino acid residues of MPPR6 were fused with DsRed. As a positive control, EMP4, a mitochondrion-targeted PPR protein (Gutiérrez-Marcos et al., 2007), was fused with green fluorescent protein (GFP) and both constructs were transiently

coexpressed in Black Mexican Sweet (BMS) cells. An overlap of the red and the green signals was observed using fluorescence microscopy, confirming mitochondrial localization of MPPR6 (Figure 8A). To investigate whether MPPR6 is also localized in the plastids, MPPR6-DsRed and cpHPS70-2-GFP, which is targeted to plastids, were transiently co-expressed in onion epidermis cells. Red and green fluorescence signals

A

B

C
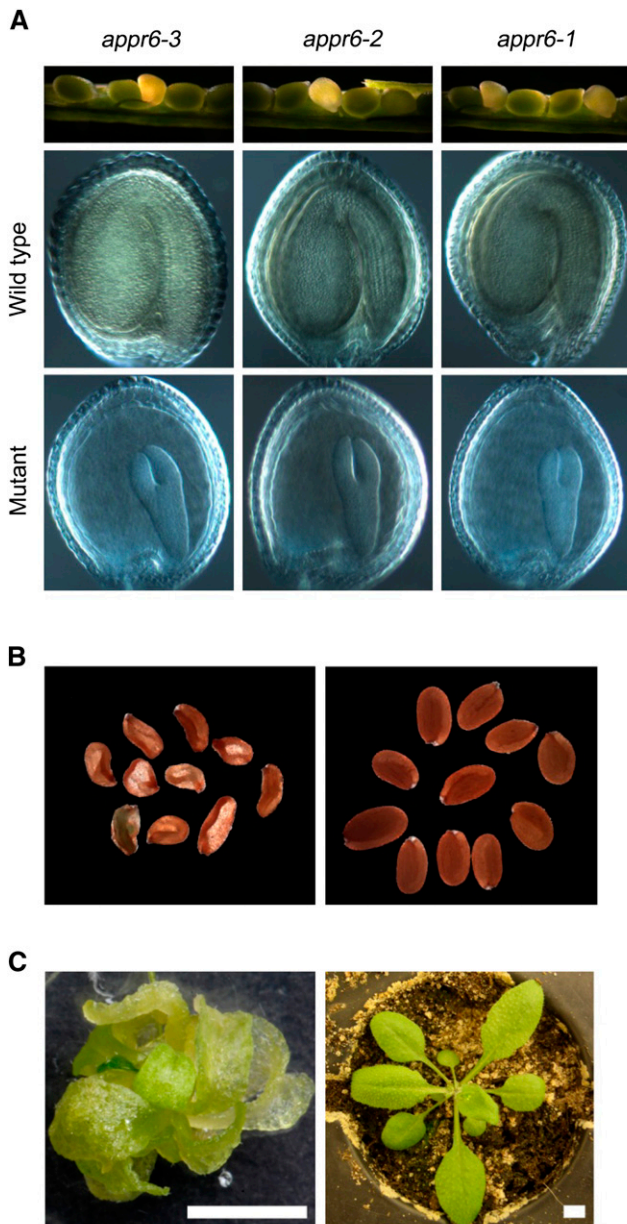
Figure 5. *appr6* Mutant Lines.

(A) Mutant phenotype of *appr6* immature seeds: from the top down, immature siliques segregating for mutant and wild-type seeds and a close-up of Hoyer's solution-cleared wild-type and mutant seeds from the corresponding siliques.

(B) Mutant (left) and wild-type (right) mature dry seeds from a plant heterozygous for *appr6-3* mutation.

(C) *appr6-3* homozygous (left) and wild-type (right) seedlings grown on MS medium and soil, respectively. Bars = 0.5 cm.

failed to overlap, indicating that MPPR6 targets only mitochondria (Figure 8B).

To confirm this further, a polyclonal antibody raised against recombinant MPPR6 was used in immunoblot analysis. In accordance with the low *MPPR6* expression, the antibody recognizes

MPPR6 only in mitochondrial protein extracts of *mppr6-Strep* overexpressing maize plants generated in this work (see Methods and Supplemental Figure 2 online) but not in the wild type (Figure 8C). For that reason, total protein extract and enriched fractions of mitochondria and chloroplasts were prepared from the overexpressor line *mppr6-Strep*. In agreement with the results of the previous subcellular localization studies, MPPR6 (~50 kD) was detectable only in the mitochondrial fraction but was absent in the chloroplast fraction and total leaf extract (Figure 8D).

MPPR6 Binds to *rps3* mRNA in Vivo and in Vitro

So far, characterized PPR proteins have been found to be involved in binding and processing of organellar RNAs. Therefore, we conducted RNA coimmunoprecipitation (Co-IP) analysis to detect a potential mitochondrial RNA associated with MPPR6 in vivo. Using polyclonal anti-MPPR6 rabbit serum, MPPR6 was immunoprecipitated from crude mitochondrial extract prepared from maize plants overexpressing *mppr6-Strep*. The RNA from the pellet was purified and polyadenylated. First-strand cDNA synthesis and subsequent cDNA amplification were performed by long-distance RT-PCR with adapter primers. As a negative control, the same Co-IP procedure was performed using preimmune serum. Two prominent RT-PCR products were obtained indicating a limited number of targets (Figure 9A). Cloning and subsequent sequencing revealed that besides the 5′ UTR of the mitochondrial *rps3* mRNA, only four clones of the plastid 23S rRNA, one of the cytoplasmic 25S rRNA, and one of unknown origin were recovered. As *rps3* was the single putative target of mitochondrial origin (Figure 9A), it appeared to be the only reasonable MPPR6 interaction partner; thus, it was selected for further investigations. Dot blot analysis of immunoprecipitated RNAs revealed that the 5′ UTR of *rps3* was indeed enriched in the pellet obtained by Co-IP with the MPPR6 antibody but absent in the pellet fraction obtained with the preimmune serum (Figure 9C).

An additional RNA Co-IP experiment was performed, in which we took advantage of the Strep-tag fused in frame to the MPPR6 protein. Crude mitochondrial protein extracts from the overexpressor *mppr6-Strep* and the wild type as negative control were subjected to a Co-IP using a strep-tactin column. Recovered RNAs were investigated by slot-blot analysis using two *rps3*-specific probes recognizing its 5′ UTR and ORF (Figure 9B), respectively, and two additional, randomly picked mitochondrial gene probes, *rps7* and *nad9*. This experiment showed a marked enrichment of the 5′UTR of *rps3* and, as expected, a slight enrichment of the middle region of the *rps3* ORF (Figure 9D). By contrast, *rps7* and *nad9* RNAs were not enriched to a similar extent, confirming the specificity by which MPPR6 recognizes *rps3* RNA.

Direct binding of MPPR6 to the 5′ UTR of *rps3* mRNA was further investigated by electrophoretic mobility shift assay (EMSA) using purified recombinant glutathione *S*-transferase (GST)-MPPR6-Strep fusion protein. In initial EMSA experiments, the binding site of MPPR6 within the coimmunoprecipitated 5′ region of *rps3* (consisting of 338 nucleotides) was narrowed down to 180 nucleotides (data not shown). This part was divided further into three overlapping regions, which were then used as probes (Figure 10A). MPPR6 most efficiently bound to the probe nearest the start codon (Figure 10C; see Supplemental Figure 3
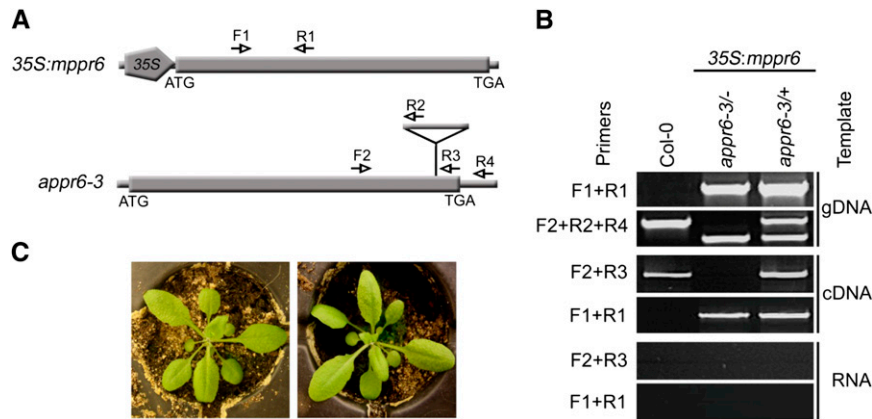
Figure 6. *MPPR6* Expression in the *appr6-3* Mutant Background.

(A) Diagram of the *35S:mppr6* transgene and *appr6-3* mutant locus. The positions of gene-specific and T-DNA primers used for genotyping and RT-PCR are shown by arrows. The T-DNA insertion is indicated by a triangle.
(B) Representative genomic and RT-PCR analysis of *35S:mppr6* harboring *appr6-3/+* and *appr6-3/−* plants and a Columbia-0 plant. Genomic PCR with *MPPR6*-specific primers confirms the success of transformation. A PCR reaction with three primers was used to distinguish between wild-type, *appr6/+*, and *appr6/−* plants. *mppr6* and *appr6* transcripts were detected by RT-PCR in leaf tissue. Genomic DNA (gDNA) contaminations in the RNA used for RT-PCR were excluded by a control PCR with RNA as template.
(C) Phenotype of 3-week-old wild-type (left) and 3-week-old *appr6-3/−* plants (right) genetically complemented by *MPPR6* expression.

online), indicating that this region, mapping from +8 to −67 with respect to the ATG start codon, most likely comprises the binding site of MPPR6. Taking into account that this region shows the highest sequence similarity to the *rps3* transcript in *Arabidopsis*, we additionally investigated binding of MPPR6 to the corresponding *rps3* region in *Arabidopsis*. In agreement with the ability of the MPPR6 protein to restore the function of the *Arabidopsis* ortholog, the *Arabidopsis* probe showed a comparably strong binding affinity to the MPPR6 protein. In addition, un-labeled maize and *Arabidopsis rps3* RNAs were able to compete efficiently with the bound maize *rps3* probe when using a 10-fold molar excess over the bound probe. Unspecific RNA probes of the mitochondrial *rps7*, *ccmC*, and *nad9* genes of similar size failed to compete efficiently (Figure 10D; see Supplemental Figure 4 online). These results clearly demonstrate that MPPR6 is spe-cifically associated with the 5′ UTR of *rps3* in vivo and is directly responsible for physical interaction as shown in vitro.

MPPR6 Is Necessary for 5′ Maturation and Translational Initiation of *rsp3* mRNA

PPR proteins are assumed to represent sequence-specific fac-tors that guide various posttranscriptionally active effector en-zymes to their targets rather than being direct effectors themselves (Barkan, 2011). To gain insight into MPPR6 function, the effect of the mutation on *rps3* processing and gene ex-pression was analyzed in the maize mutant.

Editing of maize *rps3* has not been examined so far. Ten editing sites were found in rice *rps3* (http://biologia.unical.it/py_script/log.html), which are conserved in maize as demonstrated by se-quence analysis. RT-PCR and subsequent sequencing of the *rps3* coding region revealed that all 10 editing sites within *rps3* are transmethylated in the mutant excluding a potential function in RNA editing.

Total RNA extracted from wild-type and mutant embryos were hybridized with an *rps3*-specific probe. We found that the hybridization signal of ~2.4 kb corresponding to the dicis-tronic *rps3-rpl16* transcript (Figure 11A) accumulated in the *mppr6* mutant in size comparable to that of the wild type, in-dicating that transcription and splicing of *rps3* are not affected
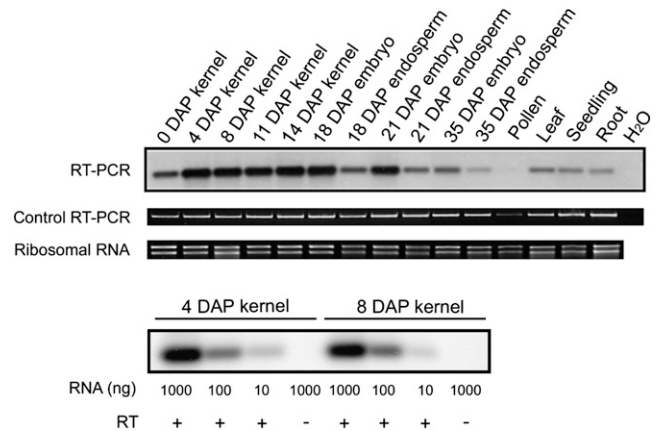
Figure 7. Expression Level of *MPPR6* in Several Maize Tissues De-termined by RT-PCR.

Total RNA from diverse maize tissues was used in reverse transcription reactions. First-strand cDNA was applied to a low cycle RT-PCR using *MPPR6*-specific primers. The resulting products were electrophoretically separated, blotted to a nylon membrane, and hybridized with a DIG-labeled *MPPR6*-specific probe (probe is diagrammed in Figure 4A). The quality check of the cDNA by a control RT-PCR using primers specific to the housekeeping maize gene *jr27* (Lorbiecke et al., 2005) is shown below. RNA quality is indicated below by staining of the rRNA with ethidium bromide. Proportional decreasing of the signal to the imputed RNA dilu-tions of two samples (4 and 8 DAP) is shown in the bottommost panel.
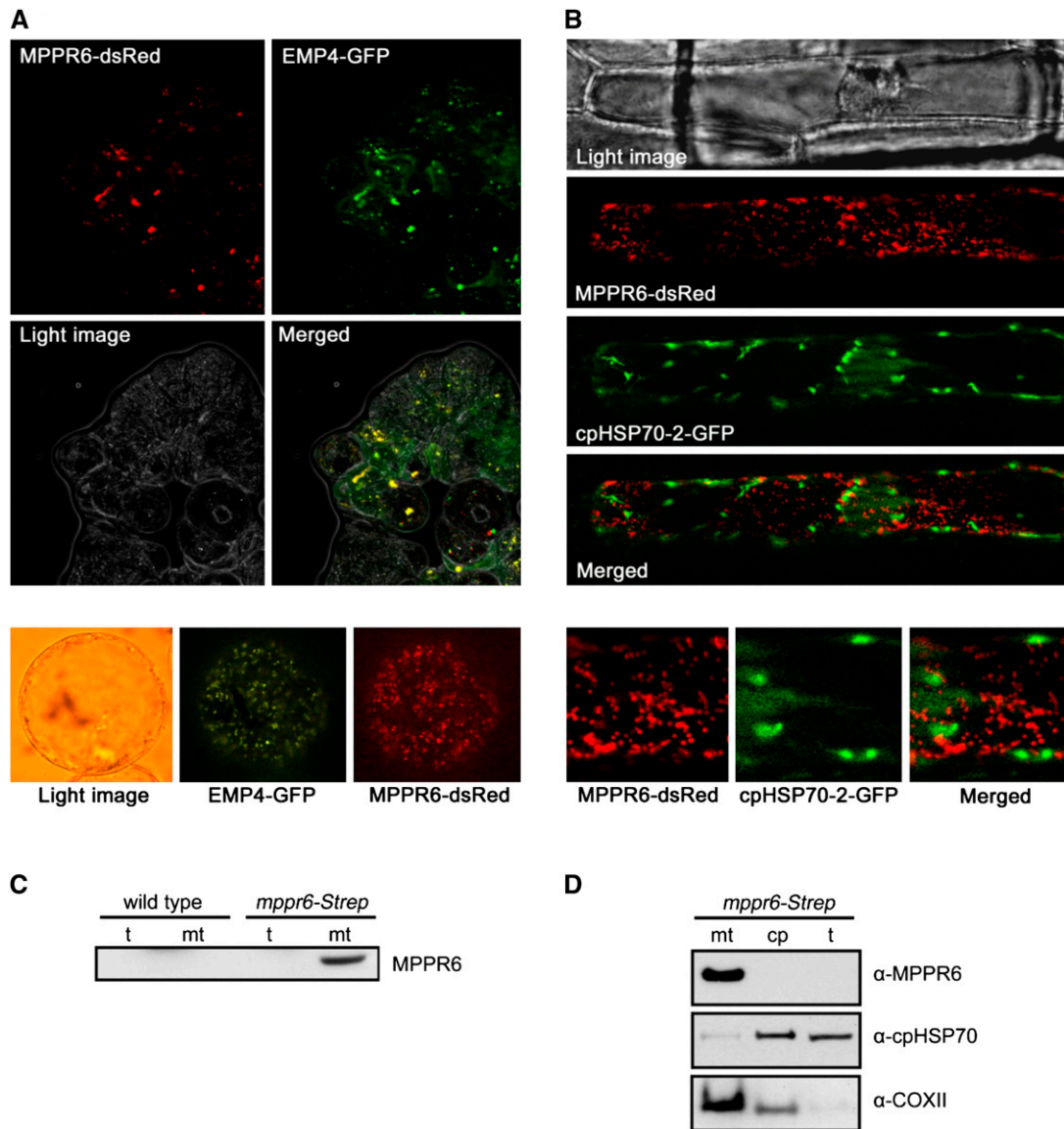
Figure 8. MPPR6 Is Targeted to Mitochondria.

(A) Subcellular localization of MPPR6 in BMS maize suspension cells. Cells were biolistically cotransformed with *Ubi:mppr6-dsRed* and *Ubi:emp4-GFP*. Micrographs show red fluorescence signals of MPPR6-dsRed, green fluorescence signals of EMP4-GFP, light image of BMS cells, and merged fluorescence of MPPR6-dsRed and EMP4-GFP. Close-up of a single transformed cell is shown below. Due to the quick movement of mitochondria within the cell caused by cytoplasmic streaming, no precise merging of both signals was possible in the close-up.

(B) Transient coexpression of MPPR6-dsRed and cpHPS70-2-GFP in onion epidermis cells. A merged image of the nonoverlapping fluorescence is shown. Close-ups of selected regions are shown below.

(C) Immunodetection of the MPPR6 protein in total protein (t) and crude mitochondria extract (mt) obtained from wild-type and *mppr6-Strep* overexpressing maize seedlings.

(D) Immunoblot analyses detected the MPPR6 protein in mitochondria but not in chloroplast (cp) fractions, both obtained from the *mppr6-Strep* overexpressor. The same filter was reprobed with chloroplast- (α-cpHPS70-2) and mitochondria-specific (α-COXII) antibodies.

by the *mppr6* mutation (Figure 11B). By contrast, the abundance of the *rps3-rpl16* transcript was considerably increased in the *mppr6* mutant compared with the wild type. This observation was confirmed by RT-PCR (see Supplemental Figure 5 online). A similar increased transcript abundance was also observed for the 18S and 26S mitochondrial rRNAs (Figure 11B), hinting at a general effect on transcript accumulation in the mutant.

The changed transcript abundance is presumably due to translation defects in agreement with the situation in chloroplasts where inhibition of translation increases levels of many transcripts (Klaff and Gruissem, 1991; Meurer et al., 2002; Kato et al., 2006).
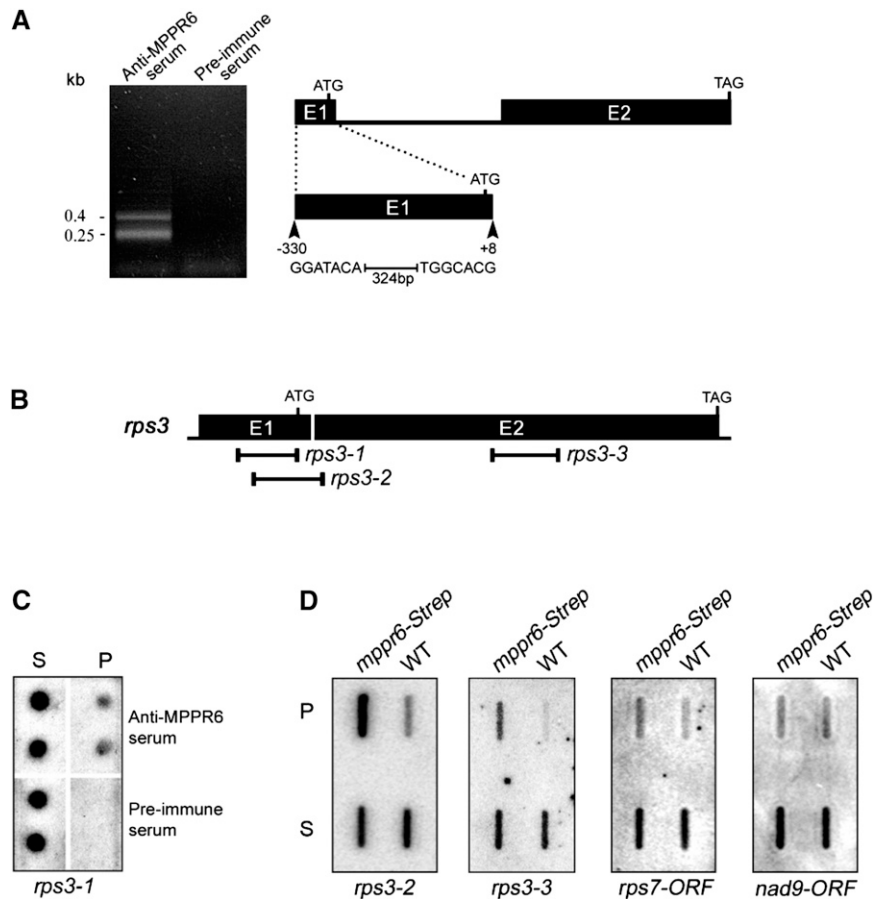
Figure 9. MPPR6 Is Associated with *rps3* in Vivo.

(A) RT-PCR products obtained from the Co-IP (left). Diagram of the intron/exon organization of *rps3* (right). Exons (E1 and E2) are shown as black bars and the intron as a black line. The *rps3* fragment found to be associated in vivo with MPPR6 is shown below as a black bar (+8 to −330, with respect to the ATG).

(B) Positions of the *rps3*-specific probes (black lines) used in the dot **(B)** and slot blot **(C)** analysis.

(C) Dot blot analysis of the coimmunoprecipitated RNAs. For the dot blot analysis, 1 µL of the RNA extracted from the pellet and the supernatant was double applied to a nylon membrane and hybridized with a ^{32}P-labeled probe specific for *rps3* (*rps3-1*, see **[B]**). RNA from the Co-IP with preimmune serum was used as negative control. P, pellet; S, supernatant.

(D) Slot blot hybridization. One-third of the RNA purified from the pellet and one-twelfth of the supernatant RNA obtained by Co-IP using wild-type (negative control) and *mppr6-strep* overexpressing plants were applied to slot blots and hybridized with the indicated ^{32}P-labeled probes (see also **[B]**). WT, the wild type.

Therefore, we checked a possible role of MPPR6 in translation of *rps3*. To achieve this goal, we generated antibodies against amino acid residues 82 to 96 of RPS3 and analyzed mitochondrial protein extracts from mutant and wild-type plants. The RPS3 protein appeared ~10 kD smaller in the mutant compared with the wild-type form of 65 kD (Figure 12A). Furthermore, levels of this truncated protein were significantly reduced in the mutant. If translation initiation was affected, we would expect that the N-terminal part of the protein would be lacking in the truncated form and that instead use of an internal in frame start codon would be responsible for the smaller version. All attempts to analyze the RPS3 protein by mass spectrometry failed. Therefore, a second antipeptide antibody against the very N terminus of RPS3 (amino acid residues 11 to 26) was generated, and mitochondrial proteins

from callus tissue were subjected to immunodetection. The serum recognized the RPS3 protein of 65 kD in the wild type as expected but failed to decorate the truncated mutant version, indicating that the N terminus rather than the C terminus is lacking (Figure 12A). This speaks in favor of the idea that the MPPR6 protein binds to the 3′ end of the *rps3* 5′ UTR to support translation initiation at its ATG start codon.

It is likely that a nonfunctional RPS3 protein generally results in impaired mitochondrial translation. For that reason, we investigated the steady state levels of mitochondrial proteins. The amounts of the mitochondrial-encoded proteins NAD9 and COXII were reduced to ~25% in the mutant, whereas peroxiredoxin-2F (PRXII F) and citrate synthase (CS), nuclear-encoded mitochondrial proteins, accumulated at levels comparably to the wild type
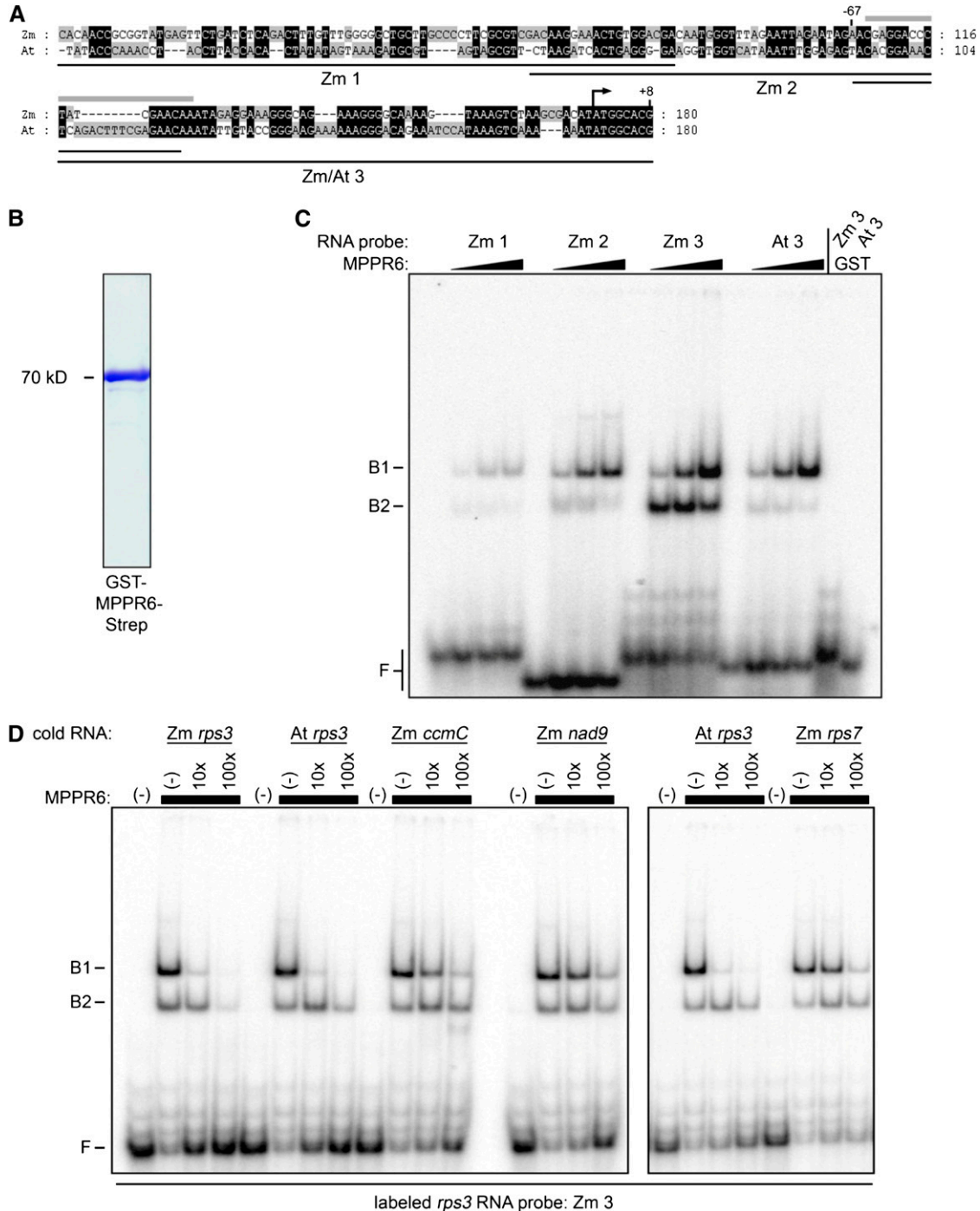
**Figure 10.** In Vitro Binding of Recombinant MPPR6 Protein to *rps3* RNA.

(A) Sequence alignment of the *rps3* 5′ region from *Arabidopsis* (At) and maize (Zm). Identical areas are highlighted in black. The sequence region of the overlapping probes (Zm 1, 2, and 3 and At 3) used in the EMSA experiment **(C)** are diagrammed as black lines. The estimated MPPR6 binding site is marked by a gray bar above the sequence. The translational start is indicated by an arrow.

(B) Coomassie blue staining of a SDS-PAGE gel of the purified protein. Recombinant GST-MPPR6-Strep protein was overexpressed in *E. coli* and purified by one-step affinity chromatography via strep tag.

(C) RNA binding of purified MPPR6 protein **(B)** was demonstrated by EMSA using the radiolabeled probes indicated in **(A)**. Binding reactions contained RNA at 50 pM and MPPR6 at 0, 50, 250, and 500 nM. The concentration of purified GST protein (negative control) was 500 nM. B1 and B2, bound RNA; F, free RNA.

(D) RNA competition experiments. Diverse nonlabeled RNAs (cold RNA: Zm *rps3*, *ccmC*, *nad9*, *rps7*, and At *rps3*) were used in 10× and 100× molar excess over the radiolabeled *rps3* probe (see **[A]**, Zm 3) using 500 nM MPPR6 protein (black boxes). B1 and B2, bound RNA; F, free RNA.

[See online article for color version of this figure.]

A

B
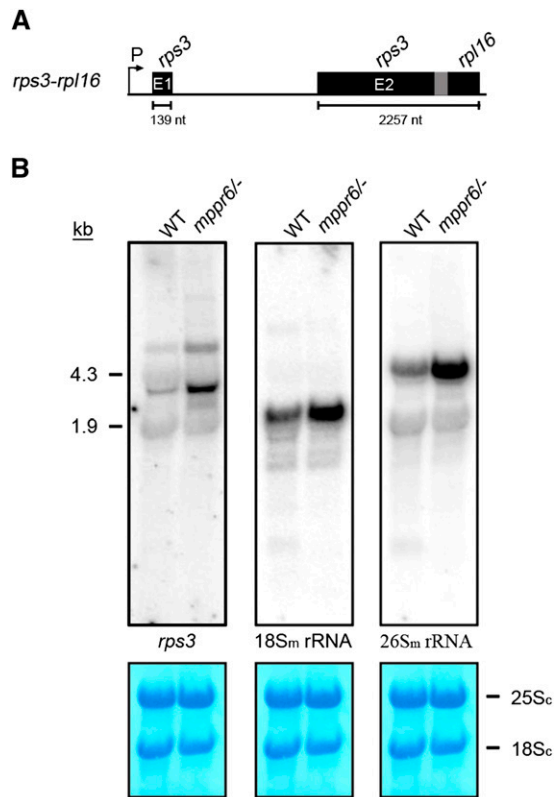
Figure 11. RNA Gel Blot Analyses of *rps3-rpl16*, 18S$_m$, and 26S$_m$ rRNAs in Wild-Type and Mutant Embryos.

(A) Organization of the dicistronic *rps3-rpl16* gene cluster (not to scale). The overlap of *rps3* and *rpl16* coding regions is shown in gray. The length of the exons is indicated below. E, exon; nt, nucleotides; P, promoter.
(B) Ten micrograms of total RNA obtained from wild-type (WT) and *mppr6* embryos was analyzed by RNA gel blot hybridization using radioactive-labeled probes specific for the second *rps3* exon and the mitochondrial 18S$_m$ or 26S$_m$ rRNAs. Methylene blue staining of cytoplasmic ribosomal 25S$_c$ and 18S$_c$ RNA is shown below. The probes used are indicated.
[See online article for color version of this figure.]

(Figure 12B). In organello protein synthesis in the presence of [^{35}S] Met revealed a similar reduction of newly synthesized mitochondrial proteins in the *mppr6* mutant (Figure 12C). Collectively, our results indicate that absence of MPPR6 causes initiation of translation downstream and in frame with the natural start codon of RPS3, which in turn results in a truncated RPS3 protein and reduced mitochondrial translation efficiency.

The question arises whether 5′ processing of *rps3* is also affected in the *mppr6* mutant. Since RNA gel blot analysis does not provide sufficient resolution to assess small size differences, we mapped the transcript ends of *rps3* by circular RT-PCR (cRT-PCR). This assay yielded two distinct amplification products of roughly 490 and 390 bp in wild type and *mppr6/−* (Figure 13A; see Supplemental Figure 6 online). Sequencing of independently cloned cRT-PCR products finally revealed size variations between the mutant and wild type. In the 390-bp products, the *rps3* 5′ end of the wild type always mapped to base position −65 nucleotides

(seven of seven clones) upstream of the start codon, which precisely coincides with the binding site of MPPR6. By contrast, in the mutant, the *rps3* 5′ end was found at quite different positions: −75 (four of seven clones), −90 (one of seven clones), and −99 (two of seven clones) (Figure 13B). In the large cRT-PCR products, all wild-type ends mapped again to the same position (−191 nucleotides, eight of eight clones), while the mutant products varied slightly in length (−194 nucleotides, seven of nine; −195 nucleotides, two of nine) (Figure 13C). As a control, the *rps3-rpl16* 3′ end position was exclusively found at +245 nucleotides downstream of the *rpl16* stop codon in both the wild type and the *mppr6* mutant (Figures 13B and 13C). In addition, *rps1* termini in the mutant and the wild type were expectably unchanged (Figure 13D), indicating that the variations of the 5′ *rps3* ends in the mutant are a specific consequence of MPPR6 absence.

The transcript ends of *rps3* were additionally determined by primer extension assay. A processing deficiency in the *mppr6/−* mutant was observed as a high molecular band likely to be the primary 5′ transcript end of *rps3*, which accumulated significantly more in the mutant compared with the corresponding primer extension product in the wild type (see Supplemental Figure 7 online), and the mature 5′ end determined by cRT-PCR (69 nucleotides upstream of the ATG start codon) failed to accumulate in the *mppr6/−* mutant. In addition, several other bands were absent in the *mppr6/−* mutant or accumulated less than in the wild type.

DISCUSSION

MPPR6 Is Essential for Seed Development

PPR mutants in land plants often result in quite diverse but not always lethal phenotypes (Lurin et al., 2004; Kocábek et al., 2006; Beick et al., 2008). Strong effects on seed development have been reported when mitochondrial localized PPR proteins are mutated (de Longevialle et al., 2007; Gutiérrez-Marcos et al., 2007). MPPR6 was shown to be important for maize seed development, since kernels are stunted and impaired in their ability to germinate in *mppr6* mutants. Bright-field imaging revealed abnormalities of the WIG formation in the *mppr6* BETL at an early stage of seed development. The BETL, the lowermost cell layer of the endosperm, is located in the immediate vicinity of the pedicel and mediates the connection between maternal and filial tissue. The most basal cell layer of the BETL is characterized by WIGs, which are labyrinth-like cell wall proliferations. By increasing the plasma membrane region, the WIGs are thought to facilitate the transfer of solutes from the maternal pedicel to the endosperm, required for seed development (Thompson et al., 2001). Therefore, normal differentiation and function of WIGs is a prerequisite for normal grain development and filling. It has been demonstrated that structural aberrations of the WIGs in the BETL at an early stage of seed development resulted later in severe seed phenotypes (Costa et al., 2003; Gutiérrez-Marcos et al., 2007; Kang et al., 2009). Furthermore, Kang et al. (2009) have shown an accumulation of mitochondria close to the WIGs, postulating a functional relationship between WIGs and mitochondria. Taking all this into account, we postulate that the
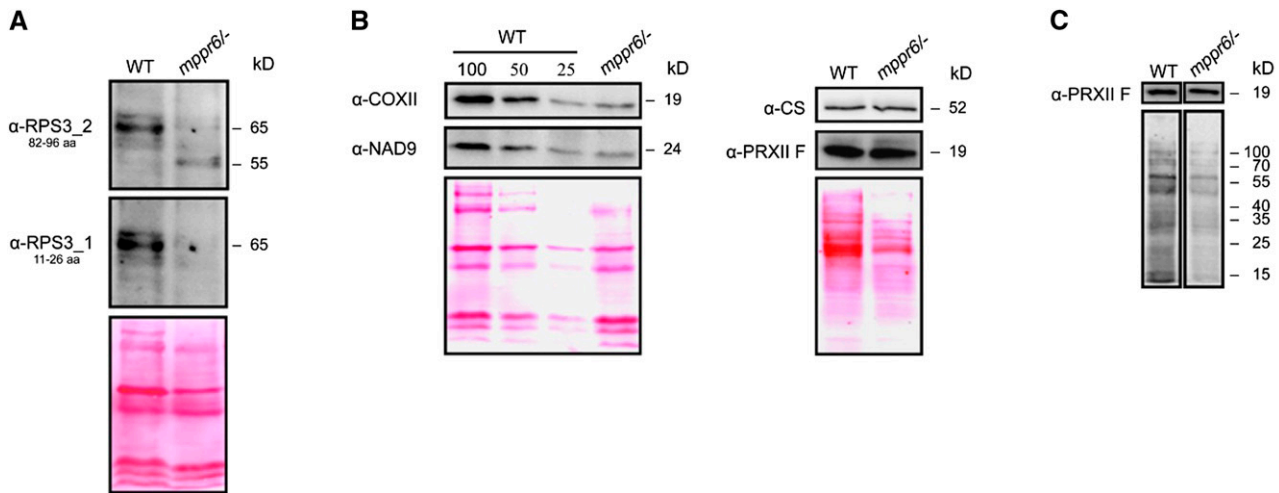
Figure 12. Disruption of MPPR6 Causes Truncation of the RPS3 Protein and a General Translational Deficiency.

(A) Immunodetection of RPS3. Twenty micrograms of mitochondrial protein extracted from wild-type (WT) and *mppr6/−* callus tissue were separated by SDS-PAGE, blotted on a nitrocellulose membrane, and consecutively probed with affinity purified anti-RPS3 antibodies raised against amino acids 82 to 96 (top panel) or 11 to 26 (middle panel). Ponceau staining of the membrane-bound proteins is shown in the panel below.

(B) Left: Dilutions of membrane protein extracts from wild-type mitochondria were compared with the *mppr6/−* mutant using antibodies raised against the mitochondria-encoded proteins NAD9 and COXI. 100% corresponds to 20 µg of mitochondrial protein. Right: Immunodetection of the nucleus-encoded mitochondrial proteins PRXII F and CS in soluble extracts from *mppr6* mutant and wild-type mitochondrial.

(C) In organello translation of wild-type and *mppr6/−* mitochondria after inhibition of cytoplasmic translation traces using cycloheximide. The same filter was probed with anti-PRXII F antibody.

[See online article for color version of this figure.]

---

observed reduction of translation efficiency in mitochondria of *mppr6* plants and therefore decreased energy supply could result in deficient WIG formation, which in return could lead to a lack of nutrient transport and cause the described poor grain filling with concomitant germination impairments. As mitochondria are essential for development and growth, the pronounced dwarfism of rescued *mppr6* plants could also be explained by aforementioned mitochondrial malfunction.

MPPR6 Is a Mitochondrial *rps3* RNA Binding Protein

PPR proteins massively emerged during endosymbiosis in plant organelles and mainly exert their functions in fast evolving and defined posttranscriptional processes (Barkan, 2011) and are therefore expected to diverge rapidly. Sequence specificity is thought to be generally conferred by recognizing defined RNA segments in coding and noncoding regions. With exception of endonucleolytic activity of DYW motif–containing PPR proteins in vitro, an enzymatic function has not yet been described for members of this protein family (Okuda et al., 2006), indicating that they likely act in concert with RNA-modifying factors.

Co-IP experiments in combination with RT-PCR were performed to identify the mitochondrial RNA target of MPPR6 in vivo. Along with the mitochondrial *rps3* 5′ UTR, only plastid and cytoplasmic rRNAs as well as a sequence of unknown origin were obtained. Nonmitochondrial RNAs very likely represent contaminations due to their high abundance and/or similar target sequences. Several lines of evidence, such as dot and slot blot analysis, in vitro RNA binding studies, a failure to process the 5′

rps3 RNA efficiently, accumulation of 5′ truncated RPS3 protein, mitochondrial translation deficiencies, and seed lethality, demonstrate the specific function of MPPR6 in *rps3* binding and expression. Misexpression of *rps3* fully explains the *mppr6* phenotype, again suggesting that *rps3* is the only target of MPPR6, although we cannot rule out that additional mitochondrial RNAs of presumably low abundance are recognized by MPPR6.

The Structure and Function of MPPR6 Protein Is Conserved among Land Plants

In *Arabidopsis*, only one close homolog of *MPPR6*, termed *APPR6*, is present. According to a sequence-based phylogenetic analysis of rice and *Arabidopsis* gene families (O'Toole et al., 2008) for more than 80% of the PPR proteins orthologs exist in both species. Using the relational database POGs (http://plantrbp.uoregon.edu/), a putative orthologous protein in rice (OPPR6) was found. Owing to the high sequence similarity of nearly 97% between the rice and maize protein, we postulated that APPR6 represents the orthologous protein in *Arabidopsis*. In favor of this idea, a highly conserved PPR motif structure and a mitochondrial transit peptide was predicted for all three putative orthologous proteins and confirmed for MPPR6 (Figure 8).

Similar to *emp4* mutants affected in a mitochondrial PPR protein and showing pleiotropic effects on RNA levels (Gutiérrez-Marcos et al., 2007), *mppr6* and *appr6* mutations cause a conditionally lethal seed phenotype in both maize and *Arabidopsis*. A functional conservation between the maize and
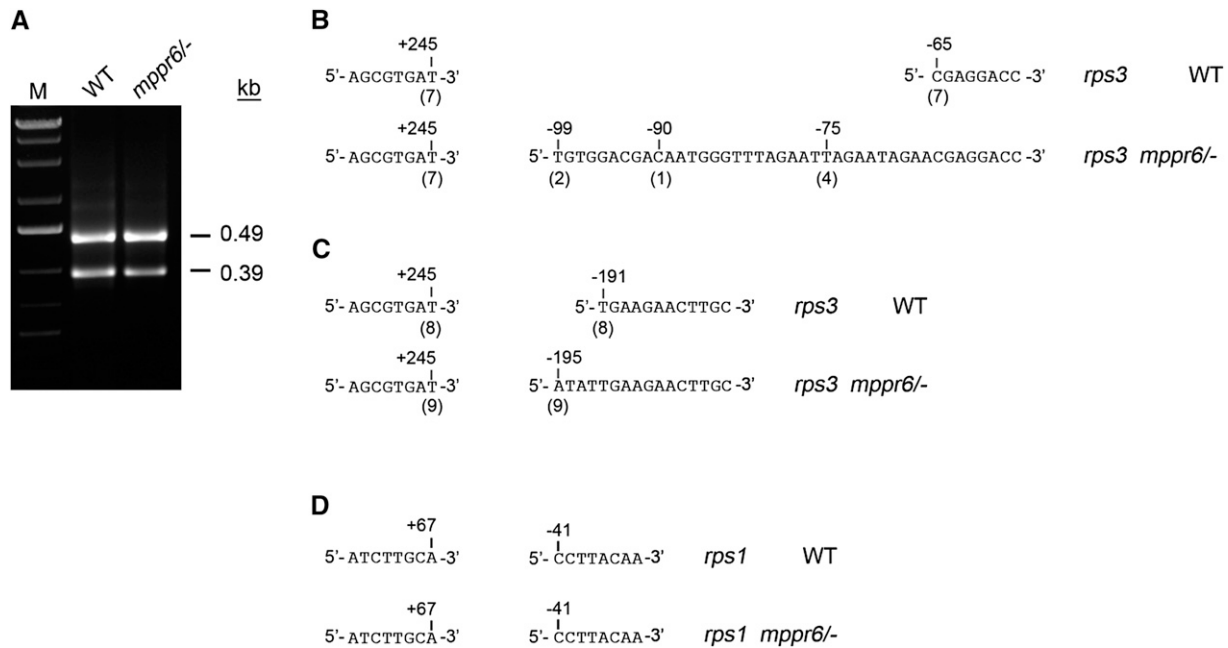
Figure 13. cRT-PCR Mapping of 3′ and 5′ *rps3* Termini in the Wild Type and *mppr6/−* Mutant.

(A) *rps3* transcript analysis using cRT-PCR. Products of circular RT-PCR were separated on 2% agarose gels, extracted, and cloned into pGEM T vector. Sequence results of independently cloned products are shown in **(B)** and **(C)**. WT, the wild type.

(B) and **(C)** *rps3* ends found in the 0.39- and 0.49-kb cRT-PCR products, respectively. The 5′ transcript ends are indicated relative to the start codon, whereas the position of the 3′ ends is shown in respect to the stop codon. The number of clones sequenced with each of the indicated ends is shown below in brackets.

(D) Control cRT-PCR of *rps1* transcripts. Obtained products were sequenced directly.

Arabidopsis protein was investigated by different methods. First, we showed that heterologous expression of MPPR6 in the corresponding *Arabidopsis appr6* mutant restored the wild-type phenotype, demonstrating a conserved function of the ortologous proteins in monocots and dicots (Figure 6C). Second, the ability of the MPPR6 to bind to the conserved target efficiently in both maize and *Arabidopsis* 5′ UTR of *rps3* was confirmed by gel shift assays, indicating that the structural features of MPPR6 and APPR6 are also conserved among land plants despite the recent burst of PPR proteins and fast evolving UTR sequences in plant organelles (Greiner et al., 2008). Third, predominant expression of both *MPPR6* and *APPR6* during early seed development demonstrates a conserved importance during this stage (Figure 7; see Supplemental Figure 8 online). Conservation of PPR function between relatively closely and distantly related species has already been shown for MRL1 and CRR4 (Okuda et al., 2008; Johnson et al., 2010). Here, we provide evidence for a conserved PPR function across a wide phylogenetic distance.

Binding of MPPR6 to the *rps3* 5′ UTR Assists 5′ Maturation

The 5′ transcript termini of *rps3* were mapped by cRT-PCR and primer extension assay. Both methods showed a processing deficiency in the *mppr6/−* mutant. However, these methods seemed to differ in their sensitivity of mapping 5′ RNA isoforms. Whereas cRT-PCR appeared to amplify shorter *rps3* transcripts preferentially, primer extension proved to detect much larger ends.

Furthermore, cRT-PCR detects only processed termini containing 5′ monophosphates, whereas in the primer extension, all kinds of transcripts could serve as a template regardless of whether they have been processed or not; thus, the primary transcript ends and possible degradation products would also be detected explaining the complexity of the primer extension products obtained. Furthermore, both methods could be affected by complex secondary structure in the RNA, which would stop the reverse transcription, resulting in absence of expected products. As primer extension assay includes an extended primer annealing step, during which secondary structure formation could occur, this experiment seems to be more sensitive to RNA folding than cRT-PCR.

Since the mature 5′ UTR in the mutant was extended by only several nucleotides, we assume that the target site is recognized and cleaved by an endonuclease rather than protected against exonucleolytic cleavage. Alternatively, unspecific endo- or exonucleolytic cleavage might take place randomly at secondary structure-free regions resulting in 5′ ends of different lengths in the mutant (Stoppel and Meurer, 2012). Consistent with this, the fully processed 5′ end of the wild type precisely coincides with the MPPR6 binding site. We used m-fold (http://mfold.rna.albany.edu) to predict the secondary structures of the differently processed wild-type and mutant *rps3* 5′ region. Interestingly, a hairpin structure occurred in the correctly processed *rps3* 5′ UTR (see Supplemental Figure 9 online), which is recognized by MPPR6. The secondary structures of the three different 5′ UTR versions found in the *mppr6* mutant proved to be more complex.

So far, only for the plastid PPR protein, PPR10, the exact RNA binding site of 17 nucleotides within overlapping 5′ and 3′ regions of chloroplast mRNAs has been defined (Prikryl et al., 2011). Questions related to the precise physical interaction between MPPR6 and its target will be subjected in future studies.

MPPR6 Facilitates Translation Initiation of *rps3*

Factors involved in initiation and control of plant mitochondrial translation remain elusive. In contrast with the eubacterial ancestor, mitochondria have lost typical Shine Dalgarno sequences and ribosomal binding sites cannot be unambiguously classified (Hazle and Bonen, 2007). Loss of these binding sites has been presumably compensated for by the evolution of many more UTR-specific PPR and other proteins allowing individualized regulation of mitochondrial gene expression. It has recently been shown that an unfolded state of RNA near the ATG start codon in Shine-Dalgarno sequence-free mRNAs in bacteria and organelles is the major requirement for efficient start codon recognition and translation initiation (Scharff et al., 2011). Secondary structures in the *rps3* 5′ UTR are therefore likely to prevent translation initiation by masking the start codon. Thus, it is tempting to speculate that MPPR6 binding loosens up the secondary structure in the 5′ region of the *rps3* mRNA, thereby facilitating ribosome recruitment and ensuring free access to the correct start codon. As a consequence of the absence of the MPPR6 protein in the mutant, the correct ATG is inaccessible; thus, an alternative start codon in a hairpin-free environment further downstream might be used, resulting in the observed truncated MPPR6 protein, which is lacking the N terminus. Since in mitochondria, ATG, GGG, AAU, GUG, or ACG is used as a start codon (Giegé and Brennicke, 2001), the N terminus of the mutant protein could not be determined with certainty.

Binding of the plastid PPR10 protein to the 3′ UTR of *atpI* transcript possibly hampers an exonuclease from continuing digestion at the binding site (Prikryl et al., 2011). Binding to the overlapping 5′ UTR of *atpH* mRNA is thought to unwind RNA to allow ribosomal binding. Similar to PPR10, a dual function in translational activation and 5′ maturation of a mitochondrial mRNA has been established for MPPR6. Interestingly, these dual functions evolved many times independently and in both plant organelles, hinting at a general principle of action for PPR proteins. Structure analysis also indicates that correct processing minimizes RNA folding around the start codon and therefore supports the action of MPPR6 in facilitating initiation of translation.

The observed mitochondrial translation deficiencies, reduced amounts of mitochondrial encoded proteins, and seed lethality in the *mppr6* mutant are likely based on the production of only truncated RPS3 proteins, which do not appear in the wild type because of efficient translation initiation at the inherent start codon. RPS3 is essential in *Escherichia coli* and part of the30S ribosomal subunit (http://www.shigen.nig.ac.jp/ecoli/pec/index.jsp). It is added to the 16S rRNA at the last step of 30S subunit assembly (Culver and Noller, 1999). The plastid RPS3 protein was also shown to be essential in tobacco (*Nicotiana tabacum*; Fleischmann et al., 2011), indicating that the mitochondrial RPS3 version is essential as well. This is supported by the fact that deletion mutations within the *rps3* gene in maize lead to a drastic reduction of mitochondrial protein synthesis along with massive growth impairments of heteroplasmic plants, whereas in homoplasmic individuals, the mutation proved to be kernel lethal (Hunt and Newton, 1991; Newton et al., 1996). Thus, absence of functional RPS3 is anticipated to result in mitochondrial translation deficiency. In the *mppr6* mutant, mitochondrial translation is considerably reduced but not missing completely, as demonstrated by immunoblots and in organello protein synthesis. Residual activity of the truncated RPS3 protein and/or the production of traces of full-length RPS3 could account for the fact that basal mitochondrial translation principally occurs in *mppr6*.

The discovery of the essential and conserved functions of MPPR6-related proteins among land plants demonstrates the specificity by which mitochondrial *rps3* gene expression is affected despite the rapid divergence of organellar UTRs. This implies an important role of MPPR6 during evolution. The recruitment of PPR and other proteins may offer the possibility of regulating expression in a gene-specific manner as has been demonstrated recently for the chloroplast PrfB3 protein (Stoppel et al., 2011). A dual role of a PPR protein in RNA processing and translation has been evolved independently and in different organelles, indicating a general principle of action during endosymbiosis. We anticipate that future research on PPR proteins will shed new light on the functional coevolution with their RNA targets.

METHODS

Plant Material and Growth Conditions

The mutant collection consisting of 27,500 maize (*Zea mays*) lines in which an endogenous *Mu* element had been allowed to transpose at high frequency was created by Biogemma using a *Mu* transposon line (provided by B. Taylor, Commonwealth Scientific and Industrial Research Organization, Canberra, Australia). The *Mu* line was crossed with maize hybrids developed by Limagrain to increase plant vigor and adaptation to European environmental conditions. Screening for defective kernels was performed visually on 22,000 F2 seeds; 6000 seed mutants were identified, 1200 of which showed an endosperm phenotype. Three hundred mutants showing a good 3:1 seed phenotype and stability of the phenotype over three generations were selected for further characterization and gene cloning. The maize lines A188 and H99 were additionally used in this study. Plants were grown in the field or in a greenhouse at 25°C, with 16 h light and a relative humidity of 55 to 95%. For DNA, RNA, and protein isolation, plant tissues were frozen in liquid nitrogen immediately after harvesting and stored at −70°C until needed.

Maize BMS cell suspension culture was used for transient biolistic transformation. The cells were cultivated in MS medium (Murashige and Skoog, 1962) supplemented with 5.98 mM L-Gln, 1.3 mM Pro, 0.67 mM Asn, 2 mg/L 2,4-D, and 30 g/L Suc at 26°C in the dark with shaking (70 rpm). BMS cells were subcultured every week in fresh medium.

To obtain 7-d-old etiolated seedlings for mitochondria isolation, surface-sterilized kernels were germinated on water-soaked paper towels under sterile conditions in the dark at 26°C.

For embryo rescue experiments, embryos were dissected from surface-sterilized 18 DAP mutant and wild-type kernels and transferred to half-strength MS medium. Rescued individuals were transferred to soil once they reached the three-leaf stage and were grown in the greenhouse in the conditions described above.

Arabidopsis thaliana lines SALK_045714 (*appr6-1*), SALK_091917 (*appr6-2*), and SALK_061950 (*appr6-3*) obtained from the Salk Institute and Columbia-0 wild type were germinated on soil or half-strength MS medium supplemented with 1.5% Suc at 23°C, with a relative humidity of 50% and a 15-h photoperiod. Heterozygous plants were identified by screening immature siliques for the presence of 25% defective seeds following self-pollination and PCR genotyping. For microscopy studies, immature seeds were cleared with Hoyer's solution as described by Liu and Meinke (1998) and examined using a Zeiss Axioscope microscope equipped with differential interference contrast optic. Mature dried seeds were visualized under dark-field illumination. Images were captured and processed using the Zeiss AxioVision camera and AxioVision software (release 4.6.3).

Fixation and Embedding of Maize Kernels

The 12 DAP mutant and wild-type kernels were trimmed on both sides parallel to the embryo axis and incubated for 16 h at 4°C in 100 mM phosphate buffer, pH 7.2, containing 4% (w/v) paraformaldehyde and 0.1% (w/v) glutaraldehyde. After two washing steps (15 min each) in ice-cold 100 mM phosphate buffer, pH 7.2, kernels were dehydrated in a graded ethanol series (40 min/change) to 100%, which was then replaced by xylene. Kernels were finally embedded in Paraplast Plus (Carl Roth). The samples were sliced into 12-μm-thick sections, placed onto silicon-coated glass slides, and incubated at 42°C overnight. After paraffin removal and rehydration, sections were stained either with Azure B, pH 4.0, for 3 min or periodic acid Schiff's reagent (Carl Roth) according to the manufacturer's instructions.

Isolation of an Additional *mppr6* Allele and Allelism Test

An additional *Mu* insertion event was isolated at Biogemma. Screening for *Mu* insertions in *MPPR6* was performed on F1 plant material, and genotyping was confirmed in the F2 progeny. A PCR-based method was performed, using a transposon terminal inverted repeat–specific primer, OmuA, and *MPPR6*-gene specific primers designed in the first half of the gene (PPR_R03 and PPR_F03). One additional mutant allele was identified, J0487, with insertion at nucleotide + 394 in the ORF of the *MPPR6* gene. The putative allelic line J0487, which showed a mutant *mppr6-1*–like seed phenotype, was renamed *mppr6-2*.

To determine genetic allelism between *mppr6-1* and *mppr6-2*, 20 phenotypically wild-type kernels from a segregating ear of each mutant line were sown on soil. Seedlings were genotyped by genomic PCR using the terminal inverted repeat–specific primer Muoligo2 in combination with mppr6_1fw (for *mppr6-1*) or mppr6_2rev (for *mppr6-2*). Some of the genomic DNA samples were additionally investigated by DNA gel blots. Crosses were then performed between *mppr6-1/+* and *mppr6-2/+* plants. The phenotype of the resulting ears was analyzed.

Cloning of *MPPR6* and cDNA Isolation

Total RNA from immature mutant kernels of two segregating sibling ears and wild-type kernels of a single sibling wild-type ear was extracted as described previously (Kluth et al., 2002). cDNA synthesis was performed according to the SMART RACE cDNA amplification kit instructions (Clontech). For both 3′ and 5′ RACE, the universal primer provided with the kit was combined with the *Mu*-specific primer Muoligo1. The nested round PCR was performed using the nested universal primer from the kit and Muoligo2. RACE products were electrophoretically separated on agarose gel and candidate bands present in the mutant samples but absent in the wild-type were eluted using the NucleoSpin Extract II kit (Machery-Nagel). The DNA was finally cloned into the pCR 2.1-TOPO vector (Invitrogen) and sequenced.

To obtain a full-length *mppr6* cDNA clone, a kernel cDNA population was generated using the SMART RACE cDNA amplification kit (Clontech) and total RNA isolated as described above. The mppr6_3fw and mppr6_3rev primers were designed on the genomic clone (MAGIv4_67802) and used to amplify the complete ORF of *MPPR6*. To obtain the 5′ and 3′ UTR, the universal primer was combined with mppr6_4fw and mppr6_4rev primers, respectively. A nested PCR round was performed using the nested universal primer in combination with mppr6_5fw and mppr6_5fw primers for the 5′ and 3′ RACE, respectively.

Cosegregation Analysis

Genomic DNA was extracted from leaf samples of wild-type and heterozygous *mppr6* sibling maize plants using the Plant Genomic DNA Mini Kit (Avegene). Genomic PCR was performed using ~100 ng genomic DNA and primers Muoligo2 and mppr6_1fw. For DNA gel blot analysis, 10 μg of *Sac*I-digested genomic DNA was electrophoretically separated on 0.8% agarose gel. DNA was transferred to a neutral nylon membrane (Hybond-NX; GE Healthcare) by capillary blotting with 20× SSC. Digoxigenin (DIG)-labeled *MPPR6*-specific probe was generated with the PCR DIG probe synthesis kit (Roche). Hybridization was performed according to the DIG Application Manual for Filter Hybridization (Roche). Target-probe hybrids were detected in a chemiluminescent reaction with CSDP (Roche) as a substrate and visualized on x-ray film.

Complementation

The *MPPR6* ORF was amplified using *Pfu* polymerase (Fermentas) and primers mppr6_3fw and mppr6_7rev. The PCR product was digested with *Bam*HI and *Xba*I and cloned into the *Bam*HI and *Xba*I sites of pCHF5 (gift of C. Fankhauser, University of Geneva, Switzerland). The resulting vector was transformed into *Agrobacterium tumefaciens* GV3101pMP90 (Koncz and Schell, 1986) and used for floral dip transformation of homozygous *Arabidopsis* plants as described by Clough and Bent (1998). Resulting seeds were sown on soil, and transgenic plants were selected by spraying the seedlings with aqueous solution of 250 mg/L phosphinothricin and 0.1% (v/v) Tween 20.

Generation of Transgenic Maize Plants

For generation of transgenic maize plants overexpressing *mppr6-Strep*, the ORF of *MPPR6* was amplified (primers: mppr6_3fw and mppr6_9rev), digested with *Bam*HI, and inserted into the *Bam*HI sites of pUbi:cas (Dirk Becker, University of Hamburg). The resulting construct, *pUbi:mppr6-Strep*, was used for generation of transgenic maize plants by stable biolistic transformation of embryogenic calli from a cross between A188 × H99 as described previously (Brettschneider et al., 1997). T0 progeny of putative transgenic, phosphinothricin-resistant plants were verified by DNA and RNA gel blot analysis according to the DIG Application Manual for Filter Hybridization.

RT-PCR

Tissues from the inbred maize line A188 were used to obtain total RNA as described previously (Kluth et al., 2002). Removal of genomic DNA contamination was performed by treatment with RNase-free DNase I (Fermentas) according to the recommended protocol. One microgram of DNA-free RNA was reverse transcribed with PrimeScript reverse transcriptase (Takara Bio) according to the manufacturer's directions of the SMART RACE cDNA amplification kit (Clontech). Three microliters of the 10-fold diluted reverse transcription reaction were used in a low-cycle (25)

PCR with *Taq* DNA polymerase (Fermentas) and the *MPPR6*-specific primers: mppr6_6fw and mppr6_6rev. One-tenth of the RT-PCR products was separated by agarose gel electrophoresis and blotted on neutral nylon membrane (Hybond-NX; GE Healthcare) by capillary transfer with 20× SSC. DIG probe labeling, hybridization, and detection were performed as described above.

For cRT-PCR, 10 μg of total RNA obtained from wild-type and *mppr6* mutant callus tissue were self-ligated using T4 RNA Ligase 1 (NEB). One-tenth of the circular RNA was subjected to reverse transcription reaction using the AMV RT (Fermentas) and gene-specific primer (rps3-rpl16_5fw), followed by two rounds of PCR with nested primers (for first-round PCR, rps3-rpl16_5fw and rps3_5rev; for second-round PCR, rps3-rpl16_6fw and rps3_6rev). Abundant cRT-PCR products were cut out from the agarose gel, purified, cloned into pGEM T vector, and sequenced. For better resolution, cRT-PCR products were additionally separated on denaturing 5% polyacrylamide gels containing 8 M urea. Electrophoresis was performed in 1% TBE buffer. cRT-PCR products were visualized after staining gels with ethidium bromide.

RNA Gel Blot Analysis

Total RNA was extracted using TRIzol reagent (Invitrogen) according to the manufacturer's instructions. Electrophoresis and RNA gel blotting were performed as described previously (Meurer et al., 2002). Hybridization was performed with ExpressHyb buffer (Clontech) and radioactive-labeled antisense 80-mers (see Supplemental Table 1 online) according to the manufacturer's instructions. Blots were analyzed with a phosphor imaging system (Typhoon; Amersham Biosciences).

Protein Analysis and Antibody Production

For isolation of total protein, leaf material was ground in liquid nitrogen and resuspended in isolation buffer (100 mM Tris-HCl, pH 8.0, 150 mM NaCl, 5 mM EGTA, 5 mM EDTA, 10 mM DTT, 0.5% [v/v] Triton X-100, and Complete Protease Inhibitor Cocktail Tablets [Roche]), and after centrifugation at 18,000*g* for 20 min, the supernatant was collected. To obtain mitochondrial proteins, crude mitochondria were resuspended in lysis buffer (30 mM HEPES-KOH, pH 7.7, 10 mM Mg acetate, 60 mM K acetate, 2 mM DTT, and 0.5% Nonidet P-40, supplemented with Complete Protease Inhibitor Cocktail Tablets) and lysed by a 30-min incubation on ice interrupted by occasional short vortexing. Membrane proteins were separated from the soluble ones by centrifugation at 20,800*g* for 30 min. Proteins were separated by SDS-PAGE, transferred into nitrocellulose membrane (Protran; Whatman) using semidry Electrophoretic Transfer Cell (Bio-Rad), and stained with Ponceau solution (0.1% [w/v] Ponceau S and 5% [v/v] acetic acid). Antibodies were used at the following dilutions: anti-MPPR6 rabbit, anti-RPS3_1 rabbit, and anti RPS3_2 rabbit 1:500 each; anti-NAD9 rabbit (Lamattina et al., 1993) 1:50,000; anti-COXII hen (Agrisera) 1:1000; anti-cpHSP70-2 rabbit (Agrisera) 1:2000; anti-PRXII F rabbit (Finkemeier et al., 2005) 1:5000; anti-CS rabbit (kindly provided by Iris Finkemeier, Ludwig-Maximillians-University Munich) 1:10,000. Signals were visualized using chemiluminescence. For antibody production, the amino acid residues 60 to 489 of MPPR6 were fused with a C-terminal His$_6$ tag using the pET30a+ vector (Novagen) and expressed in *Escherichia coli* strain BL 21 (DE3). The recombinant protein was purified under denaturing conditions on a nickel-nitrilotriacetic acid agarose column (Qiagen) and used for the generation of antibodies in rabbits at the Eurogentec's antibody facility.

Two antipeptide antibodies with specificity for RPS3 (amino acids 82 to 96, LKRRDKSRPGKDKGR, and amino acids 11 to 26, RLDLNRSSDPSRFSDY) were generated in rabbits and affinity purified by Eurogentec.

Subcellular Localization

The signal sequence of *MPPR6* (amplified with primers mppr6_3fw/rev) and the ORF of *EMP4* (amplified with primers emp4_1fw/rev) were inserted into *Ubi*:*dsRed* (constructed by R.B.) and *Ubi*:*GFP* (Lorbiecke et al., 2005), respectively. BMS cells or onion epidermis were biolistically cotransformed as described previously (Lorbiecke et al., 2005) using the resulting constructs *Ubi*:*mppr6-dsRed* and *Ubi*:*emp4-GFP*, or *Ubi*:*mppr6-dsRed* and *Ubi*:*cpHSP70-2-GFP* (kindly provided by Jantjeline Kluth, University of Hamburg, Germany), respectively. Eighteen hours later, the transient coexpression was visualized by fluorescence microscopy using a Zeiss AX10 ImagerZ1 ApoTome. The emission for dsRed was visualized at 570 to 640 nm and for GFP at 500 to 550 nm. The AxioVision 4.8 software was used for subsequent image processing.

Co-IP and Identification of MPPR6 Target Mitochondrial RNA

An enriched mitochondrial fraction was obtained from etiolated MPPR6-overexpressing maize seedlings as described previously (Takenaka and Brennicke, 2007). The crude mitochondrial pellet was resuspended in ice-cold lysis buffer (30 mM HEPES-KOH, pH 7.7, 10 mM Mg acetate, 60 mM K acetate, 2 mM DTT, and 0.5% Nonidet P-40, supplemented with Complete Protease Inhibitor Cocktail Tablets). Lysis of mitochondria was performed by two freeze/thaw cycles, followed by 30-min incubation on ice and several short vortexing steps. The lysate was then clarified by centrifugation at 20,800*g* for 15 min at 4°C and placed on ice.

Protein A Dynabeads (100 μL; Invitrogen) was washed twice in 0.5 mL of Co-IP buffer (150 mM NaCl, 20 mM Tris-HCl, pH 7.5, 1 mM EDTA, 0.5% Nonidet P-40, and Complete Protease Inhibitor Cocktail Tablets) and finally resuspended in 100 μL of the same buffer. Forty microliters of anti-MPPR6 or preimmune rabbit serum was added to the washed Protein A Dynabeads and incubated for 2 h at 4°C with rotation. After three washes with Co-IP buffer, the beads were resuspended in 800 μL of Co-IP buffer supplemented with RNase Inhibitor (Fermentas). One hundred microliters of mitochondrial extract (~1 mg protein) was added to the mixture from the previous step and incubated at 4°C overnight with rocking. Beads were collected by magnetic separation; the resulting supernatant was used for RNA extraction and subsequent dot blot hybridization. The beads were washed six times in 1 mL of Co-IP buffer, resuspended in 200 μL of Co-IP buffer supplemented with SDS to 1% and 10 mM EDTA, and incubated for 30 min at 55°C. RNA from each pellet or supernatant was phenol-chloroform extracted, ethanol-precipitated, and resuspended in 10 μL of water. Three microliters of the RNA obtained from the pellet was used in a poly(A) tailing reaction using *E. coli* Poly(A) Polymerase (NEB) according to the manufacturer's instructions. The polyadenylated RNA was reverse transcribed and subsequently amplified by a long-distance RT-PCR following the Super SMART PCR cDNA Synthesis Kit protocol (Clontech). RT-PCR products were cloned into pCR 2.1-TOPO vector (Invitrogen) and sequenced.

Immunoprecipitation of strep-tagged proteins was performed with 1 mg of mitochondrial protein using a Strep-Tactin column (IBA) according to the manufacturer's instructions. Washing and RNA extraction were performed as described above. For slot blot hybridizations, one-third of the pellet RNA and one-twelfth of the supernatant RNA were spotted onto nylon membranes and hybridized with the ^{32}P-labeled probes.

For dot blot hybridization, 1 μL of RNA purified from the pellet or the supernatant was applied to a nylon membrane and hybridized with ^{32}P-labeled *rps3* probe (Sauter, 1997) generated by a random priming method using the Prime It II DNA labeling kit (Stratagene).

Expression and Purification of Recombinant MPPR6

To generate a GST-MPPR6-Strep fusion protein, the coding sequence of *MPPR6* corresponding to the mature protein (excluding the predicted transit

sequence) was amplified by RT-PCR using primers mppr6_8fw and mppr6_8rev and inserted into the high-level expression vector pET41b+ after digestion with *Spe*I and *Xho*I. The resulting plasmid was introduced into *E. coli* strain Bl21pLysS (Novagen). Cells were grown in Luria-Bertani medium supplemented with kanamycin at 37°C to an OD_{600} of 0.7. After induction of protein synthesis by addition of isopropyl-β-D-thiogalactopyranoside, the culture was incubated for 4 h at 37°C. Cells were then lysed by sonication in strep-washing buffer (IBA) supplemented with 10% (v/v) Sarkosyl and Complete Protease Inhibitor Cocktail Tablets. The postcentrifugation supernatant was filtered through a 0.45-μm filter, diluted 1:5 with Strep-washing buffer supplemented with 2% Triton X-100 and 0.1% CHAPS, and incubated for 1 h in Strep-Tactin-Macroprep (IBA). Washing steps were performed with Strep-washing buffer lacking detergents. The GST-MPPR6-Strep-Fusion protein was eluted with strep-elution buffer supplemented with 30% glycerol. Protein concentration was determined by Bradford assay using BSA as standard. Protein purity was controlled by SDS-PAGE and subsequent Coomassie Brilliant Blue staining.

EMSA and in Organello Translation

RNAs were generated by in vitro transcription using T7 RNA Polymerase (Fermentas) according to the manufacturer's instructions. PCR products containing the T7 promoter were used as template. Reactions (25 μL) were performed in binding buffer composed of 40 mM Tris, pH 7.5, 100 mM NaCl, 0.1 mg/mL BSA, 4 mM DTT, and 0.5 mg/mL heparin at 25°C for 20 min. Protein and RNA concentrations are indicated in Figure 10. Samples were separated on a nondenaturing 4% polyacrylamide (29:1 acrylamide: bis-acrylamide) gel prepared in 0.5× TBE buffer. Gels were dried and analyzed with a phosphor imaging system (Typhoon).

In organello translation was performed as described previously (Grohmann, 1996).

Sequence Analysis

cDNA clones and PCR fragments were sequenced using the ABI Prism Big Dye reaction kit and ABI Prism sequencer (Applied Biosystems). Sequence data were analyzed using the programs included in DNASTAR 4.05 software package. PPR domains were identified using the Scan-Prosite tool of the ExPASy Proteomics Server (http://www.expasy.ch/tools/scanprosite/). The subcellular localization was determined using TargetP (Emanuelsson et al., 2000) and Predotar (http://urgi.versailles.inra.fr/predotar/predotar.html) (Small et al., 2004). For the search of putative orthologous protein groups, thePlantRBP/POGs database (http://plantrbp.uoregon.edu/) was used. Alignment was calculated with ClustalW2 (http://www.ebi.ac.uk/Tools/clustalw2/index.html) (Larkin et al., 2007) and manually edited using GeneDoc 2.6.002 (Nicholas and Nicholas, 1997).

Accession Numbers

Sequence data for *mppr6* cDNA can be found in the GenBank database under accession number HQ534069. Sequences of the maize, rice (*Oryza sativa*), and *Arabidopsis* PPR proteins shown in Figure 4 can be found in the GenBank database under accession numbers GI:313851107, GI:115455503, and GI:334183972, respectively.

Supplemental Data

The following materials are available in the online version of this article.

Supplemental Figure 1. Phenotype and Segregation of *mppr6*.

Supplemental Figure 2. Molecular Analysis of *mppr6-strep* Transgenic Plants.

Supplemental Figure 3. MPPR6 Binds to 5′ UTR of *rps3* RNA at High Salt Conditions.

Supplemental Figure 4. Unlabeled Competitor RNA.

Supplemental Figure 5. Analyses of *rps3* Transcripts.

Supplemental Figure 6. *Rps3* cRT-PCR Products Separated on Polyacrylamide Gel.

Supplemental Figure 7. Mapping of *rps3* 5′ Termini by Primer Extension Assay.

Supplemental Figure 8. *APPR6* Expression Profile Determined by the *Arabidopsis* eFP Browser.

Supplemental Figure 9. Secondary Structure of *rps3* 5′ UTRs Determined by M-Fold.

Supplemental Table 1. Names and Sequences of Used Primers.

AUTHOR CONTRIBUTIONS

N.M., R.B., J.M., U.W., and V.G. designed the research. N.M. performed the research. N.M., J.M., R.B., and V.G. analyzed data. N.M. and J.M. wrote the article.

REFERENCES

Barkan, A. (2011). Expression of plastid genes: Organelle-specific elaborations on a prokaryotic scaffold. Plant Physiol. **155:** 1520–1532.

Beick, S., Schmitz-Linneweber, C., Williams-Carrier, R., Jensen, B., and Barkan, A. (2008). The pentatricopeptide repeat protein PPR5 stabilizes a specific tRNA precursor in maize chloroplasts. Mol. Cell. Biol. **28:** 5337–5347.

Bentolila, S., Knight, W., and Hanson, M. (2010). Natural variation in Arabidopsis leads to the identification of REME1, a pentatricopeptide repeat-DYW protein controlling the editing of mitochondrial transcripts. Plant Physiol. **154:** 1966–1982.

Brettschneider, R., Becker, D., and Lörz, H. (1997). Efficient transformation of scutellar tissue of immature maize embryos. Theor. Appl. Genet. **94:** 737–748.

Cai, W., Okuda, K., Peng, L., and Shikanai, T. (2011). PROTON GRADIENT REGULATION 3 recognizes multiple targets with limited

similarity and mediates translation and RNA stabilization in plastids. Plant J. **67:** 318–327.

Chateigner-Boutin, A.L., des Francs-Small, C.C., Delannoy, E., Kahlau, S., Tanz, S.K., de Longevialle, A.F., Fujii, S., and Small, I. (2011). OTP70 is a pentatricopeptide repeat protein of the E subgroup involved in splicing of the plastid transcript *rpoC1*. Plant J. **65:** 532–542.

Chateigner-Boutin, A.L., Ramos-Vega, M., Guevara-García, A., Andrés, C., de la Luz Gutiérrez-Nava, M., Cantero, A., Delannoy, E., Jiménez, L.F., Lurin, C., Small, I., and León, P. (2008). CLB19, a pentatricopeptide repeat protein required for editing of *rpoA* and *clpP* chloroplast transcripts. Plant J. **56:** 590–602.

Clough, S.J., and Bent, A.F. (1998). Floral dip: A simplified method for *Agrobacterium*-mediated transformation of *Arabidopsis thaliana*. Plant J. **16:** 735–743.

Costa, L.M., Gutierrez-Marcos, J.F., Brutnell, T.P., Greenland, A.J., and Dickinson, H.G. (2003). The *globby1-1* (*glo1-1*) mutation disrupts nuclear and cell division in the developing maize seed causing alterations in endosperm cell fate and tissue differentiation. Development **130:** 5009–5017.

Culver, G.M., and Noller, H.F. (1999). Efficient reconstitution of functional *Escherichia coli* 30S ribosomal subunits from a complete set of recombinant small subunit ribosomal proteins. RNA **5:** 832–843.

de Longevialle, A.F., Meyer, E.H., Andrés, C., Taylor, N.L., Lurin, C., Millar, A.H., and Small, I.D. (2007). The pentatricopeptide repeat gene *OTP43* is required for *trans*-splicing of the mitochondrial *nad1* Intron 1 in *Arabidopsis thaliana*. Plant Cell **19:** 3256–3265.

Emanuelsson, O., Nielsen, H., Brunak, S., and von Heijne, G. (2000). Predicting subcellular localization of proteins based on their N-terminal amino acid sequence. J. Mol. Biol. **300:** 1005–1016.

Finkemeier, I., Goodman, M., Lamkemeyer, P., Kandlbinder, A., Sweetlove, L.J., and Dietz, K.J. (2005). The mitochondrial type II peroxiredoxin F is essential for redox homeostasis and root growth of *Arabidopsis thaliana* under stress. J. Biol. Chem. **280:** 12168–12180.

Fleischmann, T.T., Scharff, L.B., Alkatib, S., Hasdorf, S., Schöttler, M.A., and Bock, R. (2011). Nonessential plastid-encoded ribosomal proteins in tobacco: A developmental role for plastid translation and implications for reductive genome evolution. Plant Cell **23:** 3137–3155.

Giegé, P., and Brennicke, A. (2001). From gene to protein in higher plant mitochondria. C. R. Acad. Sci. III **324:** 209–217.

Greiner, S., Wang, X., Herrmann, R.G., Rauwolf, U., Mayer, K., Haberer, G., and Meurer, J. (2008). The complete nucleotide sequences of the 5 genetically distinct plastid genomes of *Oenothera*, subsection *Oenothera*: II. A microevolutionary view using bioinformatics and formal genetic data. Mol. Biol. Evol. **25:** 2019–2030.

Grohmann, L. (1996). *In organello* protein synthesis. Methods Mol. Biol. **49:** 391–397.

Gutiérrez-Marcos, J.F., Dal Prà, M., Giulini, A., Costa, L.M., Gavazzi, G., Cordelier, S., Sellam, O., Tatout, C., Paul, W., Perez, P., Dickinson, H.G., and Consonni, G. (2007). *empty pericarp4* encodes a mitochondrion-targeted pentatricopeptide repeat protein necessary for seed development and plant growth in maize. Plant Cell **19:** 196–210.

Hammani, K., des Francs-Small, C.C., Takenaka, M., Tanz, S.K., Okuda, K., Shikanai, T., Brennicke, A., and Small, I. (2011). The pentatricopeptide repeat protein OTP87 is essential for RNA editing of *nad7* and *atp1* transcripts in *Arabidopsis* mitochondria. J. Biol. Chem. **286:** 21361–21371.

Hattori, M., Miyake, H., and Sugita, M. (2007). A Pentatricopeptide repeat protein is required for RNA processing of *clpP* Pre-mRNA in moss chloroplasts. J. Biol. Chem. **282:** 10773–10782.

Hazle, T., and Bonen, L. (2007). Comparative analysis of sequences preceding protein-coding mitochondrial genes in flowering plants. Mol. Biol. Evol. **24:** 1101–1112.

Hölzle, A., Jonietz, C., Törjek, O., Altmann, T., Binder, S., and Forner, J. (2011). A RESTORER OF FERTILITY-like PPR gene is required for 5′-end processing of the nad4 mRNA in mitochondria of *Arabidopsis thaliana*. Plant J. **65:** 737–744.

Hunt, M.D., and Newton, K.J. (1991). The NCS3 mutation: Genetic evidence for the expression of ribosomal protein genes in *Zea mays* mitochondria. EMBO J. **10:** 1045–1052.

Johnson, X., Wostrikoff, K., Finazzi, G., Kuras, R., Schwarz, C., Bujaldon, S., Nickelsen, J., Stern, D.B., Wollman, F.A., and Vallon, O. (2010). MRL1, a conserved pentatricopeptide repeat protein, is required for stabilization of *rbcL* mRNA in *Chlamydomonas* and *Arabidopsis*. Plant Cell **22:** 234–248.

Jonietz, C., Forner, J., Hildebrandt, T., and Binder, S. (2011). RNA PROCESSING FACTOR3 is crucial for the accumulation of mature ccmC transcripts in mitochondria of Arabidopsis accession Columbia. Plant Physiol. **157:** 1430–1439.

Jonietz, C., Forner, J., Hölzle, A., Thuss, S., and Binder, S. (2010). RNA PROCESSING FACTOR2 is required for 5′ end processing of *nad9* and *cox3* mRNAs in mitochondria of *Arabidopsis thaliana*. Plant Cell **22:** 443–453.

Kang, B.-H., Xiong, Y., Williams, D.S., Pozueta-Romero, D., and Chourey, P.S. (2009). *Miniature1*-encoded cell wall invertase is essential for assembly and function of wall-in-growth in the maize endosperm transfer cell. Plant Physiol. **151:** 1366–1376.

Kato, K., Ishikura, K., Kasai, S., and Shinmyo, A. (2006). Efficient translation destabilizes transcripts in chloroplasts of *Chlamydomonas reinhardtii*. J. Biosci. Bioeng. **101:** 471–477.

Kiesselbach, T.A. (1949). The Structure and Reproduction of Corn. (Cold Spring Harbor, NY: Cold Spring Harbor Laboratory Press).

Klaff, P., and Gruissem, W. (1991). Changes in chloroplast mRNA stability during leaf development. Plant Cell **3:** 517–529.

Kluth, A., Sprunck, S., Becker, D., Lörz, H., and Lütticke, S. (2002). 5′ Deletion of a *gbss1* promoter region from wheat leads to changes in tissue and developmental specificities. Plant Mol. Biol. **49:** 669–682.

Kobayashi, K., Kawabata, M., Hisano, K., Kazama, T., Matsuoka, K., Sugita, M., and Nakamura, T. (2012). Identification and characterization of the RNA binding surface of the pentatricopeptide repeat protein. Nucleic Acids Res. **40:** 2712–2723.

Kocábek, T., Repková, J., Dudová, M., Hoyerová, K., and Vrba, L. (2006). Isolation and characterization of a novel semi-lethal *Arabidopsis thaliana* mutant of gene for pentatricopeptide (PPR) repeat-containing protein. Genetica **128:** 395–407.

Koncz, C., and Schell, J. (1986). The promoter of T$_L$-DNA gene *5* controls the tissue-specific expression of chimaeric genes carried by a novel type of *Agrobacterium* binary vector. Mol. Gen. Genet. **204:** 383–396.

Koprivova, A., des Francs-Small, C.C., Calder, G., Mugford, S.T., Tanz, S., Lee, B.R., Zechmann, B., Small, I., and Kopriva, S. (2010). Identification of a pentatricopeptide repeat protein implicated in splicing of intron 1 of mitochondrial nad7 transcripts. J. Biol. Chem. **285:** 32192–32199.

Kotera, E., Tasaka, M., and Shikanai, T. (2005). A pentatricopeptide repeat protein is essential for RNA editing in chloroplasts. Nature **433:** 326–330.

Lamattina, L., Gonzalez, D., Gualberto, J., and Grienenberger, J.M. (1993). Higher plant mitochondria encode an homologue of the nuclear-encoded 30-kDa subunit of bovine mitochondrial complex I. Eur. J. Biochem. **217:** 831–838.

Larkin, M.A., et al. (2007). Clustal W and Clustal X version 2.0. Bioinformatics **23:** 2947–2948.

Liu, C.M., and Meinke, D.W. (1998). The *titan* mutants of *Arabidopsis* are disrupted in mitosis and cell cycle control during seed development. Plant J. **16:** 21–31.

Liu, Y., He, J., Chen, Z., Ren, X., Hong, X., and Gong, Z. (2010). ABA overly-sensitive 5 (ABO5), encoding a pentatricopeptide repeat protein required for cis-splicing of mitochondrial nad2 intron 3, is involved in the abscisic acid response in Arabidopsis. Plant J. **63:** 749–765.

Lorbiecke, R., Steffens, M., Tomm, J.M., Scholten, S., von Wiegen, P., Kranz, E., Wienand, U., and Sauter, M. (2005). Phytosulphokine gene regulation during maize (*Zea mays* L.) reproduction. J. Exp. Bot. **56:** 1805–1819.

Lowe, J., and Nelson, O.E. (1946). Miniature seed-a study in the development of a defective caryopsis in maize. Genetics **31:** 525–533.

Lurin, C., et al. (2004). Genome-wide analysis of *Arabidopsis* pentatricopeptide repeat proteins reveals their essential role in organelle biogenesis. Plant Cell **16:** 2089–2103.

Meierhoff, K., Felder, S., Nakamura, T., Bechtold, N., and Schuster, G. (2003). HCF152, an *Arabidopsis* RNA binding pentatricopeptide repeat protein involved in the processing of chloroplast *psbB-psbT-psbH-petB-petD* RNAs. Plant Cell **15:** 1480–1495.

Meurer, J., Lezhneva, L., Amann, K., Gödel, M., Bezhani, S., Sheramети, I., and Oelmüller, R. (2002). A peptide chain release factor 2 affects the stability of UGA-containing transcripts in *Arabidopsis* chloroplasts. Plant Cell **14:** 3255–3269.

Millar, A.H., Heazlewood, J.L., Kristensen, B.K., Braun, H.-P., and Møller, I.M. (2005). The plant mitochondrial proteome. Trends Plant Sci. **10:** 36–43.

Murashige, T., and Skoog, F. (1962). A revised medium for rapid growth and bio assays with tobacco tissue cultures. Physiol. Plant. **15:** 473–497.

Newton, K.J., Mariano, J.M., Gibson, C.M., Kuzmin, E., and Gabay-Laughnan, S. (1996). Involvement of S2 episomal sequences in the generation of NCS4 deletion mutation in maize mitochondria. Dev. Genet. **19:** 277–286.

Nicholas, K.B., and Nicholas, H.B.J. (1997). GeneDoc: A tool for editing and annotating multiple sequence alignments. EMBNEW. NEWS **4:** 14.

Okuda, K., Habata, Y., Kobayashi, Y., and Shikanai, T. (2008). Amino acid sequence variations in Nicotiana CRR4 orthologs determine the species-specific efficiency of RNA editing in plastids. Nucleic Acids Res. **36:** 6155–6164.

Okuda, K., Nakamura, T., Sugita, M., Shimizu, T., and Shikanai, T. (2006). A pentatricopeptide repeat protein is a site recognition factor in chloroplast RNA editing. J. Biol. Chem. **281:** 37661–37667.

O'Toole, N., Hattori, M., Andres, C., Iida, K., Lurin, C., Schmitz-Linneweber, C., Sugita, M., and Small, I. (2008). On the expansion of the pentatricopeptide repeat gene family in plants. Mol. Biol. Evol. **25:** 1120–1128.

Pfalz, J., Bayraktar, O.A., Prikryl, J., and Barkan, A. (2009). Site-specific binding of a PPR protein defines and stabilizes 5′ and 3′ mRNA termini in chloroplasts. EMBO J. **28:** 2042–2052.

Prikryl, J., Rojas, M., Schuster, G., and Barkan, A. (2011). Mechanism of RNA stabilization and translational activation by a pentatricopeptide repeat protein. Proc. Natl. Acad. Sci. USA **108:** 415–420.

Pusnik, M., and Schneider, A. (2012). A trypanosomal pentatricopeptide repeat protein stabilizes the mitochondrial mRNAs of *cytochrome oxidase subunit* 1 and 2. Eukaryot. Cell **11:** 79–87.

Royo, J., Gomez, E., and Hueros, G. (2007). Transfer cells. In Endosperm, Plant Cell Monographs, Vol. 8 (Berlin: Springer-Verlag), pp. 73–89.

Sauter, M. (1997). Differential expression of a CAK (cdc2-activating kinase)-like protein kinase, cyclins and *cdc2* genes from rice during the cell cycle and in response to gibberellin. Plant J. **11:** 181–190.

Scharff, L.B., Childs, L., Walther, D., and Bock, R. (2011). Local absence of secondary structure permits translation of mRNAs that lack ribosome-binding sites. PLoS Genet. **7:** e1002155.

Schmitz-Linneweber, C., and Small, I. (2008). Pentatricopeptide repeat proteins: A socket set for organelle gene expression. Trends Plant Sci. **13:** 663–670.

Schmitz-Linneweber, C., Williams-Carrier, R., and Barkan, A. (2005). RNA immunoprecipitation and microarray analysis show a chloroplast pentatricopeptide repeat protein to be associated with the 5′ region of mRNAs whose translation it activates. Plant Cell **17:** 2791–2804.

Schmitz-Linneweber, C., Williams-Carrier, R.E., Williams-Voelker, P.M., Kroeger, T.S., Vichas, A., and Barkan, A. (2006). A pentatricopeptide repeat protein facilitates the *trans*-splicing of the maize chloroplast *rps12* pre-mRNA. Plant Cell **18:** 2650–2663.

Small, I., Peeters, N., Legeai, F., and Lurin, C. (2004). Predotar: A tool for rapidly screening proteomes for N-terminal targeting sequences. Proteomics **4:** 1581–1590.

Small, I.D., and Peeters, N. (2000). The PPR motif - A TPR-related motif prevalent in plant organellar proteins. Trends Biochem. Sci. **25:** 46–47.

Stoppel, R., Lezhneva, L., Schwenkert, S., Torabi, S., Felder, S., Meierhoff, K., Westhoff, P., and Meurer, J. (2011). Recruitment of a ribosomal release factor for light- and stress-dependent regulation of *petB* transcript stability in *Arabidopsis* chloroplasts. Plant Cell **23:** 2680–2695.

Stoppel, R., and Meurer, J. (2012). The cutting crew - Ribonucleases are key players in the control of plastid gene expression. J. Exp. Bot. **63:** 1663–1673.

Sung, T.Y., Tseng, C.C., and Hsieh, M.H. (2010). The SLO1 PPR protein is required for RNA editing at multiple sites with similar upstream sequences in Arabidopsis mitochondria. Plant J. **63:** 499–511.

Takenaka, M., and Brennicke, A. (2007). RNA editing in plant mitochondria: Assays and biochemical approaches. Methods Enzymol. **424:** 439–458.

Thompson, R.D., Hueros, G., Becker, H., and Maitz, M. (2001). Development and functions of seed transfer cells. Plant Sci. **160:** 775–783.

Uchida, M., Ohtani, S., Ichinose, M., Sugita, C., and Sugita, M. (2011). The PPR-DYW proteins are required for RNA editing of *rps14*, *cox1* and *nad5* transcripts in *Physcomitrella patens* mitochondria. FEBS Lett. **585:** 2367–2371.

Uyttewaal, M., Mireau, H., Rurek, M., Hammani, K., Arnal, N., Quadrado, M., and Giegé, P. (2008). PPR336 is associated with polysomes in plant mitochondria. J. Mol. Biol. **375:** 626–636.